

Dear Prof. Huang,

Thank you very much for editing this paper and the authors would like to thank the reviewers for their careful evaluations and comments on our paper. We have revised the manuscript according to the reviewers' detailed comments. Please find the responses to the reviewers.

For your and the reviewers' convenience to review the changes, a copy of the text with highlighted changes (changes are in red color) is also attached here.

Thank you very much for all your help and look forward to hearing from you soon.

Sincerely,

Xuemei Wang and coauthors

Please find the following Response to the comments of reviewers.

Reviewers' comments are in plain face.

Authors' responses are in blue color.

Changes in the manuscript are in red color.

Response to the referees' comments

Response to Referee#1:

We would like to thank the reviewer for the careful evaluations and positive comments on our paper, which improved the paper so much. We have revised the manuscript according to the reviewer's detailed comments. Please find the responses to the reviewers.

Comments to the Author:

It is a pleasure to review the manuscript "Properties of aerosols and formation mechanisms over southern China during the monsoon season" by Chen et al. This manuscript addresses an important science question: what are the characteristics of size distribution and formation of atmospheric aerosols in southern China and how they are affected by local and long-range transport? Given the heavy PM concentrations in that region, answering this question has practical implications for public health. This study makes diligent use of a unique in-situ dataset, modeling, and remote-sensing products, investigates various physical and chemical mechanisms of aerosol (including secondary) formation and evolution, and provides some new insights into this scientific issue. The paper is comprehensive in its scope, well organized and well written, and the research quality is high. I suggest to accepting this manuscript after the authors clarify the following points, which are mostly minor concerns and editorial changes:

- Line 150, the model required the use of measured: did you have all those measurements from your site observations?

Response:

Yes, all of these required parameters were observed at these three sites, including ambient temperature, relative humidity, and the concentration of sulfate, nitrate and ammonium. We have added more information about chemical analysis in line 151-156:

‘The mass concentrations of six cations (Na^+ , NH_4^+ , K^+ , Ca^{2+} , Mg^{2+} , and Ca^{2+}) and seven anions (F^- , Cl^- , NO_2^- , Br^- , SO_4^{2-} , NO_3^- and PO_4^-) were analyzed using an ion chromatography (ICS-3000, DIONEX). Thermal Optical Transmittance (TOT) technique was employed to analyze the quartz filter samples to determine the mass concentrations of organic carbon (OC) and elemental carbon (EC) by the use of Sunset Laboratory OCEC Carbon Aerosol Analyzer.’

- Line 180, use of GDAS: why did you use higher resolution WRF/Chem meteorological fields in place of GDAS?

Response:

WRF model could provide higher resolution meteorological data, further to improve the dispersion simulations and lead to an overall better simulation (Stohl, 1998). In addition, a novel convective scheme has been added in the FLEXPART –WRF (Brioude et al., 2013), which also could improve the model simulation, especially for finer scale applications. So meteorological fields provided by WRF instead of GDAS were used in this study. We have added an explanation in line 205-209:

‘ The application of FLEXPART –WRF with a novel convective scheme being added improves the dispersion simulations and results in an overall better simulation, especially for finer scale applications (Brioude et al., 2013; Stohl, 1998). In this case, the region was modeled with a spatial resolution of 27×27 km and a temporal resolution of 1 hour.’

- Line 187: the sentence is confusing. It looks like you use WRF simulated fields as input to FLEXPART, which contradicts with the previous statement of using GDAS?

Response:

Just as the reviewer said, WRF simulation provided meteorological fields for ELEXPAET, while GDAS was applied by HYSPLIT. So we have deleted this sentence and just kept the previous statement in line 201-205:

‘HYSPLIT uses single air parcels to compute trajectories with the use of Global Data Assimilation System (GDAS, 1°×1°) as input data. FLEXPART, on the other hand, uses a larger number of air parcels to compute trajectories based on the meteorological predictions provided by mesoscale model WRF.’

- Line 200: Which two sites are referring to here? There are three sites listed in Table 1.

Response:

We are sorry for our imprecise statement. Actually the range of [0.52, 0.55] and [0.72, 0.76] is the range for three sites not only for two sites. We have re-written this part to avoid confusion in line 226-228:

‘In terms of the mass size distribution, the percentage of PM_{1.0} to PM₁₀ was 60.2%, 66.3% and 75.0%, and PM_{2.5} to PM₁₀ was 88.0%, 92.6%, 91.7% in GZ, ZH and JFM, respectively.’

- Line 203-208: very nice analysis!

Response: Thanks so much for the review’s acceptance.

- Line 287: something is missing the sentence “far-upwind urbanization and biomass burning”. Urbanization cannot be transported.

Response:

Thanks for the reviewer's reminder, we have added more information in line 316-319:

‘We investigated these days and find that emissions that long-range transported from far-upwind areas with highly urbanization or with the existence of biomass burning are responsible, as discussed later in this paper.’

- Line 304, "the sites": which sites? - The quality of some figures are acceptable but not very good. For instance: o Figs 3c&d: the figure labels need to be improved. It is hard to read. o Fig 4: again the x-axis label is hard to read. o Fig 6 labels need to be improved.

Response:

Thanks for pointing out this issue. The sites represent the three sites. We have clarified it in line 339-341:

‘Additionally, it was determined that during these times at the three sites there was an abnormally high amount of low cloud cover 60-70% and a relatively higher relative humidity (75~83%) (Table 2).’

Thanks so much for the review's suggestion, we have improved and re-plotted the figures in the main text.

- Line 417: a nice example of using backward trajectories to test your hypothesis!

Response: Thanks so much for the review's acceptance.

- Section 3.6: can authors elaborate on the MODIS Fire products? Are these daily products or twice a day or 8-day?

Response:

Thanks for the reviewer's suggestion, the MODIS fire products are daily products, we have provided some information about MODIS Fire products in the section 2 *Measurements and methodology* in line 184-193:

‘Aerosol optical depth (AOD), fire products including Fire Radiative Power (FRP), and Fire Quality Assurance [QA] data, were obtained from the MODIS sensors aboard both the AQUA and TERRA satellites. Specifically, we obtained the Collection 6, 3km Level 2 swath product for AOD (Remer et al., 2013), and Collection 5.1, 1km Level 2 swath products for FRP and QA (Giglio et al., 2006). The Collection 5.1 active fire products are daily products and have been improved based on the previous collection 5.0 products. All of the data are cloud-screened, with AOD data being computed using different algorithms over land and water, and the fire data using 19 different channels for quality assurance. We only accept values for FRP and Fire Count where the QA is at least 90%.’

And in line 550-555:

‘MODIS fire hotspots are not very useful in wet and tropical regions. Since MODIS fire hotspots are obstructed by both clouds and high levels of aerosols in the atmosphere, both of which are found associated with tropical forest fires. Additionally, due to the highly wet ground surface, a significant amount of the fires may low temperature and therefore not observable using the MODIS sensors (Cohen, 2014, Giglio et al., 2006; Yu et al., 2015).’

Editorial suggestions:

- Line 92: replace “The data is” by “those data were”

Response:

Thanks and we have modified it.

- Line 94: insert “of size distribution” between “characteristics” and “in”

Response:

Thanks and we have added it

- Lin 98-99: something is missing in “and the impacts mixing sea-salt and urban pollutants”

Response:

Thanks for reminding and we have added more information in line 106-107.

‘and the impacts mixing sea-salt and urban pollutants on the characteristics of aerosol size distributioin .’

- Line 103: it would be good to show photos of these sites to give an idea of site environments

Response:

Thanks for the suggestion, we have added photos of these sites in Figure 1

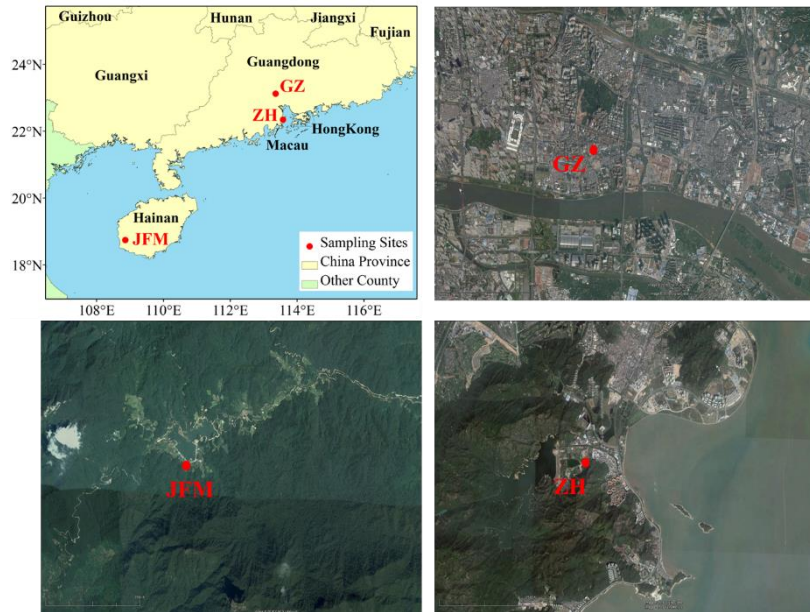


Figure 1. Location of sampling sites in Southern China: GZ (Guangzhou), ZH (Zhuhai), and JFM (Jianfeng Mountain) **and their surrounding environments**

- Line 110: replace “The first site was set at (23.12N, 113.36E), on” by “The first site (23.12N, 113.36E), is located on”

Response:

Thanks and we have modified it.

- Line 111: replace “an urban mega-city” by “a mega-city”

Response:

Thanks and we have modified it.

- Line 149: delete “to”

Response:

Thanks and we have modified it.

- Line 170: replace “All of the data is” by “All data are”

Response:

Thanks and we have modified it.

- Line 194: delete “mass”

Response:

Thanks and we have modified it.

- Line 212-213: replace “no matter what the particle size was” by “irrespective of particle size”

Response:

Thanks and we have modified it.

- Line 217: should “formed” be “from”

Response:

Thanks and we have modified it.

- Line 219: delete “with”

Response:

Thanks and we have modified it.

– Line 226: delete “of”

Response:

Thanks and we have modified it.

- Line 242: replace “showing” by “shows”

Response:

Thanks and we have modified it.

- Line 281: replace “high levels” by “high-level”

Response:

Thanks and we have modified it.

- Line 288: replace “as talked about later” by “as discussed later in this paper”

Response:

Thanks and we have modified it.

- Line 303: replace “show” by “shown”

Response:

Thanks and we have modified it.

- Line 312: replace “evidence” by “evidenced”

Response:

Thanks and we have modified it.

- Line 323: replace “of the” by “shows that”

Response:

Thanks and we have modified it.

- Line 489: delete the second “instead”

Response:

Thanks and we have modified it.

- Line 527-529: replace “Based on specific case studies, some models of the air flow, and remote sensing, the impacts of chemistry and atmospheric transport were investigated” by “These site observations, together with model simulations and Remote-sensing data, were used to investigate impacts of chemistry and atmospheric transport”.

Response:

Thanks and we have modified it.

- Line 547: delete “further”

Response:

Thanks and we have modified it.

- Line 554: be specific on “they”. What are they?

Response:

Thanks and ‘they’ represent ‘OC and EC’, we have clarified it.

Reference:

Brioude, J., Arnold, D., Stohl, A., Cassiani, M., Morton, D., Seibert, P., Angevine, W.,

- Evan, S., Dingwell, A., Fast, J.D., Easter, R.C., Pisso, I., Burkhardt, J. and Wotawa, G.: The Lagrangian particle dispersion model FLEXPART-WRF version 3.1, *Geoscientific Model Development*, 6, 1889-1904, doi:10.5194/gmd-6-1889-2013, 2013.
- Stohl, A.: Validation of the lagrangian particle dispersion model FLEXPART against large-scale tracer experiment data, *Atmospheric Environment*, 32, 4245-4264, doi:10.1016/S1352-2310(98)00184-8, 1998.
- Yu, C., Chen, L.F., Li, S.S., Tao, J.H. and Su, L.: Estimating Biomass Burned Areas from Multispectral Dataset Detected by Multiple-Satellite, *Spectroscopy and Spectral Analysis*, 35, 739-745, doi:10.3964/j.issn.1000-0593(2015)03-0739-07, 2015.

Response to Referee#2:

We would like to thank the reviewer for the careful evaluations and positive comments on our paper, which improved the paper so much. We have revised the manuscript according to the reviewer's detailed comments. Please find the responses to the reviewers.

Comments to the Author:

In this study, size distributions of chemical components of aerosols were observed at three stations located in urban, suburban, and background areas. Results were thoroughly discussed from various aspects. I think this is a nice paper, but I feel the explanations are not enough or not adequate. They should be modified before this paper is accepted for publication.

A lot of previous studies are adequately referred. But, what are new findings of this study? Results of this study may be easily imaginable based on previous studies referred in this paper. The importance and significance, and the differences from previous studies should be made insisted in the introduction.

I think one problem of this manuscript is that the overall observed data are not shown and not discussed. Are all the data obtained for the target two months those shown in Figure S1? If so, this figure should be shown in the main text and overall explanation for them are necessary at first. If it is missing, I have an impression that only the day which are easy to add explanations are picked up for analyses.

Response:

(1). A series of studies about the mass size distribution of aerosol chemical components have conducted at a specific site over Southern China during the past decade (Lan et al., 2011; Liu et al., 2008; Yang and Wenig, 2009; Zhang et al., 2015). Compared with the previous studies, this paper presents a unique combination of analytical and measurement techniques. We use measurements of chemical properties and size distribution conducted at three different functional sites, coupled with multiple modeling results, and reprocess remote sensing products using statistical methods, all in tandem with each other, which is not commonly found in other studies. Furthermore, we test our approach in Southern China, which is one of the regions of the world with the most complex meteorology, coming under the influence of the Monsoon, with shifting winds from Continental and Oceanic sources. Additionally, the season tested is a transition period, during which there were significant meteorological contributions from both remote Continental sources as well as oceanic sources. On top of this, Southern China has a combination of high temperature and relative humidity, strong radiative flux, and high oxidative capacity, leading to the promotion of significant secondary aerosol formation. This paper will provide detailed information on size-resolved aerosol chemical components and discussion on the formation mechanism in a typical region and period. We have emphasized the importance and significance in the introduction in line 84-99:

‘A series of studies about the mass size distribution of aerosol chemical components have conducted at a specific site over Southern China during the past decade (Lan et al., 2011; Liu et al., 2008; Yang and Wenig, 2009; Zhang et al., 2015). Compared with the previous studies, this paper presents a unique combination of analytical and measurement techniques. We use measurements of chemical properties and size distribution conducted at three different functional sites, coupled with multiple modeling results, and reprocess remote sensing products using statistical methods, all in tandem with each other, which is not commonly found in other studies. Furthermore, we test our approach in Southern China, which is one of the regions of the world with the most complex meteorology, coming under the influence of the Monsoon, with shifting winds from continental and oceanic sources. Additionally, the season tested is a transition period, during which there were significant meteorological contributions from both remote continental sources as well as oceanic sources. On top of this, Southern China has a combination of high temperature and relative humidity, strong radiative flux, and high oxidative capacity, leading to the promotion of significant secondary aerosol formation.’

(2). The overall observed data for the target two months were shown in Figure S1, which has now been moved into the paper as Figure 2. Additionally, all of the data obtained for the target months is displayed in line 145-150: ‘A total of 10, 8 and 20 sets of size-segregated particle samples were collected in GZ, ZH and JFM, respectively during the periods of May and June in 2010 (shown in Figure 2). A single set of sample collection lasted for approximately 24h in GZ and ZH, and 48h in JFM. Since the aerosol concentration was relatively low in remote JFM site, we extended the sampling time as long as 48h to allow the chemical components to be detected.’ and line 217-223: ‘The time series of PM₁₈ chemical compositions at the three sites during the sampling period were shown in Figure 2. The average concentration and standard deviation of PM₁₈ was 47.8±20.8, 24.3±12.1 and 8.1±2.7 μg m⁻³ in GZ, ZH and JFM, respectively. The mean and range of PM₁₈ in highly urban GZ was both higher and wider than in suburban ZH and rural JFM, with the respective ranges being 23.3~93.7, 13.3~35.1, 4.7~14.3 μg m⁻³ in the three sites. Maximum concentration was found both on 12th Jun. in GZ and ZH, while it was on 3rd Jun. in JFM (to be discussed later).’

Specific comments are as follows:

-Line 58-60 Cohen and Wang (2013) appear twice.

Response:

Thanks for pointing out that and we have deleted the repeated reference.

-Line 60-62 It may be difficult for some readers to understand modes listed here. It is better to briefly explain their definitions. Actually, this sentence is obvious because the four modes listed here (Aitken, condensation, droplet, and coarse modes) cover

almost entire aerosols.

Response:

Thanks for the suggestion and we have provided the definition for the four modes in line 59-61:

‘In the environment, the most important aerosol processes occur over the Aitken ($<0.1 \mu\text{m}$), condensation ($\sim 0.1\text{-}0.5 \mu\text{m}$), droplet ($\sim 0.5\text{-}2.0 \mu\text{m}$), and coarse ($>2.0 \mu\text{m}$) size modes (Seinfeld and Pandis, 2006)’

Just as the reviewer mentioned, the sentence is obvious because the four modes cover almost entire aerosols, what we want to emphasize is the different processes occurred on different modes as shown in line 61-63:

‘new particles are formed in the Aitken mode via condensational growth and coagulation of nucleation mode particles, and droplet mode particles are produced by in-cloud processing or aqueous reactions.’

Line 61-62 I suppose that new particles via the nucleation form in the Aitken mode, and not in the condensation mode. Do “new particles” mean those form on existing aerosols via condensation of gases?

Response:

Thanks for pointing out this issue. Just as the reviewer suggested, the new particles are formed in the Aitken mode via nucleation formation. Here, new particles mean that condensational growth and coagulation of nucleation mode particles. We have modified it in line 61-62:

‘new particles are formed in the Aitken mode via condensational growth and coagulation of nucleation mode particles’

Line 65 “Different” source types from what? What are differences?

Response:

Coarse mode aerosols usually originate from natural or mechanically produced anthropogenic sources, for example, sea spray, soil dust, dust storm, active biological aerosol (pollen, spores), etc. We have clarified this sentence in line 65-68:

‘On the other hand, coarse mode aerosols usually come from very different sources than smaller aerosols. For example, natural sources such as sea spray, dust, soil, and active biological aerosols are unique and therefore provide further information about the aerosol distribution at a given location’

Line 75-76 Pierson and Brachaczek should be (1998), not (1988).

Response:

Thanks for pointing out this mistake and we have amended it.

Line 138 What do “6 sets” correspond to? There are 7 cut-off diameters.

Response:

Thanks for pointing out this clerical error and it should be 7 sets. We have corrected it in the paper.

Line 142-143 I could not understand why number of samples becomes these number. The sampling campaign was performed for two months. 24h sampling was performed every other day in GZ and ZH. So maximum number of samples is around 30, isn't it? 48h sampling was conducted every day in JFM. Does it mean two sampling instruments were used to obtain a sample for 48h every day? How the total number of samples in JFM becomes 140 only for two months? How many days the samples were properly collected and missing? Please add more explanations to understand overall pictures of the samples used in this study.

Response:

We are sorry for our imprecise statement. The sampling was performed on a specific day, but not every other day, the specific date was shown in Figure 2. Only one instrument was operated in JFM since the concentration of aerosol was relatively lower, so we extended the sampling time as long as 48h to allow for sufficient connection of the chemical components so that they could be detected. We have clarified it in line 143-150:

‘To attain size-segregated particle samples, a 6-stage High Flow Impactor (MSP) with an airflow rate of 100 L min^{-1} was employed, with cutoff diameters (D_p) of 18 (inlet), 10, 2.5, 1.4, 1.0, 0.44 and $0.25 \mu\text{m}$. A total of 10, 8 and 20 sets of size-segregated particle samples were collected in GZ, ZH and JFM, respectively, during the periods of May to June in 2010 (shown in Figure 2). A single set of sample collection lasted for approximately 24h in GZ and ZH, and 48h in JFM. Since the aerosol concentration was relatively low in JFM, we extended the sampling time as long as 48h to make the chemical components detected.’

Line 144 Detailed information of the in-lab chemical analytical techniques is described in Zhang et al. (2013a), but at least it is necessary to mention also here which species were analyzed in this study.

Response:

We agree with the comment and we have added more information about chemical analysis in line 151-156:

‘The mass concentrations of six cations (Na^+ , NH_4^+ , K^+ , Ca^{2+} , Mg^{2+} , and Ca^{2+}) and seven anions (F^- , Cl^- , NO_2^- , Br^- , SO_4^{2-} , NO_3^- and PO_4^-) were analyzed using an ion

chromatography (ICS-3000, DIONEX). Thermal Optical Transmittance (TOT) technique was employed to analyze the quartz filter samples to determine the mass concentrations of organic carbon (OC) and elemental carbon (EC) by the use of Sunset Laboratory OCEC Carbon Aerosol Analyzer.’

Line 145-147 The background literatures should be explicitly shown here, especially for the definition of droplet particles.

Response:

Thanks for the suggestion and we have added more information in line 159-163:

‘To be consistent with the background literature (4 modes include Aitken ($<0.1 \mu\text{m}$), condensation ($\sim 0.1\text{-}0.5 \mu\text{m}$), droplet ($\sim 0.5\text{-}2.0 \mu\text{m}$), and coarse ($>2.0 \mu\text{m}$)) (Seinfeld and Pandis, 2006), and the constraints of the size bins measured in this study, we implement $2.5 \mu\text{m}$ as the cut-off size to separate fine and coarse particles, and the size bins from $0.44\text{-}1.4 \mu\text{m}$ was defined as droplet particles in this study.’

Line 155 Is it possible to ignore effects of other ions? Is it just because only these three ions were detected? Weren’t other ions used in AIM-II model, either?

Response:

Actually, the mass concentrations of six cations (Na^+ , NH_4^+ , K^+ , Ca^{2+} , Mg^{2+} , and Ca^{2+}) and seven anions (F^- , Cl^- , NO_2^- , Br^- , SO_4^{2-} , NO_3^- and PO_4^-) were analyzed in this study, as we have added the chemical analysis in section 2 *Measurements and methodology*. The possible error would be introduced due to the excluding of other ions (e.g. K^+ , Na^+ , Cl^-), but which exerted only a minor influence on the estimation of aerosol acidity due to their lower concentration. And, Yao et al. (2006) found that AIM provides the most accurate prediction compared with other models, like ISORROPIA and SCAPE2. We have added an explanation in line 163-169: ‘Although we were not able to directly measure aerosol water content, given its importance for the study here, we instead estimated the amount by the use of E-AIM model II (Clegg et al., 1998), as it provides the most accurate prediction compared with other models, like ISORROPIA and SCAPE2 (Yao et al., 2006). The input parameters of the E-AIM model II are temperature, relative humidity, strong acidity (H^+), molar concentrations of NH_4^+ , SO_4^{2-} and NO_3^- ions (Clegg et al., 1998)’ and in line 172-174: ‘The calculation of strong acidity would introduce possible errors due to the exclusion of other ions (e.g. K^+ , Na^+ , Cl^-), but which only exerted a minor influence on the estimation of aerosol acidity due to their lower concentration (Yao et al., 2006).’

Line 176-183 Differences between HYSPLIT and FLEXPART are described, but what is a specific reason why these two models were used in this study? What are expectations from these two models in the context of this study?

Response:

HYSPLIT and FLEXPART were applied to determine the origin of air masses. Furthermore, FLEXPART could identify the relative importance of source region that affected the receptor visually. We have added some information to illustrate our expectation in line 196-201:

‘Two Lagrangian particle dispersion models, the Hybrid Single Particle Lagrangian Integrated Trajectory (HYSPLIT) (Draxler and Hes, 1998) and FLEXPART coupled with The Weather and Research and Forecasting (WRF) model (FLEXPART –WRF) (Stohl et al., 1998; Brioude et al., 2013) were applied to determine the origin of air masses in this study, Compared with HYSPLIT, FLEXPART can identify the relative importance of source region that affected the receptor visually.’

Line 198-200 Does it mean that the percentages of all the samples collected at all the locations fall within such the narrow range? That is kind of incredible. Or just the averaged values shown in Table 1 fall within this range? That is nonsense. The percentages calculated for each sample should be discussed here.

Response:

Thanks for the comment. The percentage is the averaged values at the three sites shown in Table 1. We have re-written this part to avoid confusion in line 224-229:

‘Table 1 listed the average concentration of chemical components in the given size-resolved particle (PM_{1.0}, PM_{2.5} and PM₁₀) and their percentage of PM₁₀ at the three sites. In terms of the mass size distribution, the percentage of PM_{1.0} to PM₁₀ was 60.2%, 66.3% and 75.0%, and PM_{2.5} to PM₁₀ was 88.0%, 92.6%, 91.7% in GZ, ZH and JFM, respectively. When considered as a whole, it is the smaller sized particles that dominate the aerosol loading at all three of these sites.’

Line 203 What does “the majority of individual chemical species” mean? A reason of this question is because it is unclear which species were detected in this study.

Response:

Thanks for pointing out this issue. We have added more information on aerosol chemical components in line 151-156: ‘The mass concentrations of six cations (Na⁺, NH₄⁺, K⁺, Ca²⁺, Mg²⁺, and Ca²⁺) and seven anions (F⁻, Cl⁻, NO₂⁻, Br⁻, SO₄²⁻, NO₃⁻ and PO₄⁻) were analyzed using an ion chromatography (ICS-3000, DIONEX). Thermal Optical Transmittance (TOT) technique was employed to analyze the quartz filter samples to determine the mass concentrations of organic carbon (OC) and elemental carbon (EC) by the use of Sunset Laboratory OCEC Carbon Aerosol Analyzer.’ and we have clarified it in line 229-231: ‘Looking at the data on a species-by-species level, most of chemical components were concentrated in fine mode particles, which contributed at least 57% to PM_{2.5}’

Line 207-208 Again, which are “detected chemical components”?

Response:

Thanks for pointing out this issue. The detected chemical components including six cations (Na^+ , NH_4^+ , K^+ , Ca^{2+} , Mg^{2+} , and Ca^{2+}), seven anions (F^- , Cl^- , NO_2^- , Br^- , SO_4^{2-} , NO_3^- and PO_4^-) and carbonaceous aerosol (OC and EC). We have added more information on aerosol chemical components in line 151-156:

‘The mass concentrations of six cations (Na^+ , NH_4^+ , K^+ , Ca^{2+} , Mg^{2+} , and Ca^{2+}) and seven anions (F^- , Cl^- , NO_2^- , Br^- , SO_4^{2-} , NO_3^- and PO_4^-) were analyzed using an ion chromatography (ICS-3000, DIONEX). Thermal Optical Transmittance (TOT) technique was employed to analyze the quartz filter samples to determine the mass concentrations of organic carbon (OC) and elemental carbon (EC) by the use of Sunset Laboratory OCEC Carbon Aerosol Analyzer.’

Line 215-216 References of “the nature of the sources” should be shown here, especially for shipping sources. Are there any references showing shipping sources are dominant around this region?

Response:

Thanks for pointing out this issue and we have added the related references in line 241-245:

‘These findings are consistent with the nature of the sources of sulfur from industrial and power plant (Zheng et al., 2009). In addition, shipping source was becoming increasingly vital for SO_2 emission with an increment of 12% per year in this region (Lu et al., 2013; Zhou et al, 2016)’

Line 217-218 I suppose mobile vehicles are not main sources for sulfate. What is “high temperature industry”?

Response:

We agree with the comment that mobile vehicle are not the main sources of sulfate. High temperature industry represent industry and power plant. So we have re-written this sentence to avoid confusion in line 246-247:

‘Nitrate, mainly formed from the oxidation of NO_x emitted by mobile vehicles and power plants, showed a remarkable difference between urban and background site’

Line 220-221 How can rapid oxidation of precursor species be a reason of differences between urban and background sites? I suppose the phase equilibrium should be also one of important reasons of differences because nitrates would move to gas phase while transported to background areas.

Response:

We agree with that phase equilibrium is one of the important reasons in background areas. However, rapid oxidation of precursors is the main source for nitrate in urban area. So we have changed the expression in line 249-253:

‘This is consistent with its more rapid oxidation of its abundant precursor species, especially so in the urban atmosphere (Cohen et al., 2011). In addition, phase equilibrium was another important reason for the discrepancy since nitrate would tend to exist as gas phase while transported to background areas (Seinfeld and Pandis, 2006).’

Line 263-265 The percentages shown here are against what?

Response:

Thanks for pointing out this issue. We have deleted this sentence.

Line 265-266 Droplet mode nitrate is formed similarly to sulfate. Does it mean that nitrate is also formed via aqueous reactions? If so, what kind of aqueous reactions? If not, why nitrate is included in the droplet mode?

Response:

Thanks for pointing out this issue. The formation of droplet mode nitrate is unlike sulfate. Droplet mode nitrate was dominated by the heterogeneous aqueous reaction of gaseous nitric acid (HNO_3) and ammonia (NH_3) on the wet surfaces of pre-existing aerosols with ammonia-rich environment, otherwise by heterogeneous hydrolysis of N_2O_5 on the pre-existing aerosols with ammonia-poor conditions. The dissociation equilibrium of NH_4NO_3 highly depends on temperature and humidity (Stelson and Seinfeld, 1982). We have re-written these sentences in line 293-298:

‘Droplet mode nitrate was dominated by the heterogeneous aqueous reaction of gaseous nitric acid (HNO_3) and ammonia (NH_3) on the wet surfaces of pre-existing aerosols within ammonia-rich environment, otherwise by heterogeneous hydrolysis of N_2O_5 on the pre-existing aerosols within ammonia-poor conditions. The dissociation equilibrium of NH_4NO_3 highly depends on temperature and humidity (Stelson and Seinfeld, 1982).’

Line 289 What is coarse OC with a possible source of biological aerosol? Any references?

Response:

The possible source for coarse OC would be active biological aerosol, for example, pollen, spores, plant fragment. We have added more information in line 319-323:

‘Additionally, there is some coarse mode OC present in JFM, suggesting a possible source of biological aerosol (e.g. pollen, spores and plant fragment) (Heald and

Spracklen, 2009; Seinfeld and Pandis, 2006; Zhang et al., 2015), which is consistent with the large amounts of vegetation present in that region (Zhang et al., 2015).’

Line 298-301 I could not understand this sentence. How the author judged the average size was small, the particles were relatively young, and indicative of new particle formation? Are all of these coming from the fact that droplet mode sulfate accounted for about two thirds of the total mass concentration of sulfate? More detailed explanations are necessary to reinforce this discussion.

Response:

Thank you for your suggestion. After careful analysis, we admit that we could not draw this conclusion just based on the fact that droplet mode sulfate accounted for about two thirds of the total mass concentration of sulfate. Therefore, we have deleted this sentence to avoid the confusion.

Line 306-308 That is true for selected days. But, how about for days not selected? Low cloud cover 60-70% and higher relative humidity were observed only for the days selected here?

Response:

Thanks for pointing out this issue. In order to study the aqueous-phase reaction of droplet mode sulfate, cases with the air masses came from continent were excluded to avoid the effect of transported pollutants on the concentration of sulfate. Then two cases with a concentration of droplet sulfate above the mean plus one standard deviation were selected as typical cases in each site. It was found that the selected cases happened under the conditions of higher relative humidity and low cloud cover. Lower cloud cover (60-70%) and higher relative humidity were also observed for other non-selected days, which also shared with higher percentage (60% above) of sulfate in droplet mode sulfate to total sulfate but with relatively lower absolute concentrations. Therefore cases with extremely high droplet mode sulfate were selected to study, which were more obvious to observe. We have added more description in line 327-334:

‘In order to study the aqueous-phase reaction of droplet mode sulfate, cases with the air masses came from continent were excluded to avoid the effect of transported pollutants on the concentration of sulfate. Then two cases with a concentration of droplet sulfate above the mean plus one standard deviation were selected as typical cases in each site (8th and 12th May in GZ, 12th May and 1st Jun. in ZH, and 4th and 13th May 2010 in JFM), which were more obvious to observe to investigate the effect of aqueous-phase reaction in the formation of droplet mode sulfate (blue shade in Figure 2).’

Line 335 Are the words “Accumulation mode” and “condensation mode” used for the

same meaning?

Response:

The diameter for accumulation mode particles was $\sim 0.1-1\mu\text{m}$ as for WRF/Chem model, while the diameter for condensation and droplet mode was $\sim 0.1-0.5$ and $\sim 0.5-2.0\mu\text{m}$. So accumulation mode and condensation mode are not exactly the same, but the diameter for accumulation mode is between the range for condensation and droplet mode. We have clarified it in line 370-372:

‘Simulation of these conditions using WRF/Chem indicates that the rapid growth of both Aitken and accumulation ($\sim 0.1-1\mu\text{m}$) mode sulfate started at 07:00 LT and peaked at 08:00-09:00 LT’

Line 352 Is it possible to judge that fine mode chloride and sodium are coming from sea salts? Are there any anthropogenic sources of chloride and sodium in the fine mode? If chloride and sodium in the fine mode are emitted separately from different sources from sea salts, discussions on chloride depletion in the fine mode in this paragraph is not appropriate.

Response:

Thanks so much for pointing out this issue. Fine mode Na^+ and Cl^- probably came from combustion sources, e.g. biomass burning and coal combustion (Wang et al., 2005), but the contributions were insignificant since the magnitude of Na^+ and Cl^- from combustion sources is many orders of magnitude smaller than oceanic sources. Furthermore, if the biomass burning source were significant, it would clearly also show up in terms of the K^+ and BC/OC ratio, as explained later in the section **3.6 Quantifying the impacts of fires**.

We totally agree with the reviewer’s comment that the anthropogenic emissions would also affect chloride depletion in fine mode particles. So in the revised version, we introduced an indicator, concentration of chloride depletion ($[\text{Cl}_{dep}]$), to simply remove the possible effect of non-sea salt emissions. Therefore, samples with possible non-sea salt sources were excluded from analysis to avoid the effect of non-sea salt emission on chloride depletion in fine mode particles. We have clarified it in line 379-399:

‘The mass size distribution of Cl^- and Na^+ showed a similar pattern to nitrate at the three sites, peaking in coarse mode particles (Figure 5 (a-c)) with an average percentage of 43%, 62% and 43% for coarse mode Na^+ , 53%, 76% and 74% for coarse mode Cl^- in GZ, ZH and JFM, respectively, suggesting the main sea salt sources. Na^+ and Cl^- shown a bi-modal distribution in GZ, illustrating the combustion emissions, e.g. biomass burning or coal combustion for fine mode Na^+ and Cl^- (Wang et al., 2005), but the contributions were insignificant since the magnitude of Na^+ and Cl^- from combustion sources is many orders of magnitude smaller than oceanic sources. Furthermore, if the biomass burning source were significant, it would clearly

also show up in terms of the K^+ and BC/OC ratio, as explained later in the section **3.6 Quantifying the impacts of fires**.

The concentration and percentage of chloride depletion ($[Cl_{dep}]$ and $\%Cl_{dep}$) were calculated using Eq. (2-3), where $[Cl_{meas}^-]$ and $[Na_{meas}^+]$ are the measured molar concentrations of Cl^- and Na^+ , respectively; 1.174 was the molar ratio of Cl^- to Na^+ in sea water (Yao et al., 2003b).

$$[Cl_{dep}] = 1.174[Na_{meas}^+] - [Cl_{meas}^-] \quad (2)$$

$$\%Cl_{dep} = \frac{1.174[Na_{meas}^+] - [Cl_{meas}^-]}{1.174[Na_{meas}^+]} * 100\% \quad (3)$$

The positive value of $[Cl_{dep}]$ represents chloride depletion, otherwise means the chloride enrichment, suggesting additional sources was existed for Cl^- excluding sea salt. Therefore, samples with negative $[Cl_{dep}]$ were excluded from analysis to avoid the effect of non-sea salt emission on chloride depletion.'

Line 362 What does “calculated ammonium” mean? How was it calculated?

Response:

Calculated ammonium was equal to $2*[nss-SO_4^{2-}] + [NO_3^-]$, where $[nss-SO_4^{2-}]$ and $[NO_3^-]$ represents the molar concentration of non-sea-salt SO_4^{2-} (i.e., $[nss-SO_4^{2-}] = [SO_4^{2-}] - 0.14 \times [Cl^-]$) and NO_3^- . We have added related information in line 413-416:

‘Calculated ammonium was equal to $2*[nss-SO_4^{2-}] + [NO_3^-]$, where $[nss-SO_4^{2-}]$ and $[NO_3^-]$ represents the molar concentration of non-sea-salt SO_4^{2-} (i.e., $[nss-SO_4^{2-}] = [SO_4^{2-}] - 0.14 \times [Cl^-]$) and NO_3^- (Huang et al., 2004)’

Line 381 What is another important non-linear effect? It is unreasonable to discuss reasons of percentage differences only based on humidity. A lot of other factors like emission sources on pathways should be considered.

Response:

Thanks for pointing out this issue. There are indeed three important sources of non-linearity, but we do not mention them all. First, chemical/aqueous phase non-linearity. Second, meteorological non-linearity. When the wind direction changes from ocean, to land, or to long-range transport, that the chemical compositions are different, as well as the time under which in-situ chemistry could occur. Third, emissions non-linearity. When there are fire sources, the emissions are significantly different from when there are non-fire sources, and this extends to the NO_2 emissions (and hence NO_x).

We estimated the chloride depletion in ZH and JFM when the air masses came from the ocean or continent. Actually, it didn't show much difference for %Cl_{dep} no matter where the air masses came from. We agree with the reviewer's comment that another factors like emission sources also need to be considered. So drawing the conclusion that 'suggesting another important non-linear effect between maritime aerosols and anthropogenic NO_x' just based on the percentage difference would be inadequate. Therefore we have deleted this paragraph to make the paper more robust.

Line 403 Please add the definitions of Sulfur Oxidation Ratio and Nitrogen Oxidation Ratio, and their importance in the context of this study.

Response:

The Sulfur Oxidation Ratio (SOR) and Nitrogen Oxidation Ratio (NOR), which were used to indicate the degree of transformation of secondary aerosol (Wang *et al.*, 2005). We have added related information in line 454-461:

'The Sulfur Oxidation Ratio (SOR) and Nitrogen Oxidation Ratio (NOR) are applied to indicate the degree of oxidation of SO₂ and NO₂ precursor gases (Wang *et al.*, 2005). The equations for SOR and NOR are calculated as $SOR = n\text{-SO}_4^{2-} / (n\text{-SO}_4^{2-} + n\text{-SO}_2)$ and $NOR = n\text{-NO}_3^- / (n\text{-NO}_3^- + n\text{-NO}_2)$, where $n\text{-SO}_4^{2-}$ and $n\text{-NO}_3^-$ are the molar concentrations of particulate SO₄²⁻ and NO₃⁻ and $n\text{-SO}_2$ and $n\text{-NO}_2$ are the molar concentrations of the precursor gases SO₂ and NO₂. SOR and NOR was also the highest On 12th June at the range of 0.44-1.0 μm in GZ with the value of 0.20 and 0.17, respectively'

Line 439 I cannot understand discussions around here. Why can discussions in this paragraph be a reason of long-range transport? As mentioned in the line 425-426, wind speed was very low. Isn't it possible to explain high concentrations and aging under stagnant air around urban area? Do the discussions in this paragraph enable to clearly distinguish effects of stable air and long-range transport?

Response:

Thanks for pointing out this issue. Discussion in this paragraph was only one aspect of long-range transport, the following discussions were additional evidences to support this conclusion. We clearly explain this more precisely as follows:

First, HYSPLIT and FLEXPART-WRF showed that the air flow was mostly from Southeast Asia at levels over the boundary layer, and hence had undergone long-range transport. Second, the windspeed near the surface suddenly became very low. Therefore, there had been a rapid change in the windspeed. Based on conservation laws for air mass, it would be expected for there to be some reasonable amount of mixing of the air vertically. This was consistent with the finding that some of the air which had undergone long-range transport would have mixed into the surface region. Third, the chemical concentrations of BC, OC, and K⁺ were all elevated, Na⁺ and Cl⁻ size distribution were peaked in the 1.0-1.44 μm size range, and they were bi-modal distribution in ZH, which were also consistent with a significant fire contribution.

Fourth, the time-gap between when the air parcels left Southeast Asia and arrived in Guangzhou and Zhuhai, correspond very well with times during which the EOFs over Southeast Asia showed a significantly large amount of smoke (Figure 10), which would be discussed in section 3.6. *Quantifying the impacts of fires*.

We make clear this in the text in line 495-515:

‘Except for in-situ formation, long-range transport was another impact factor. First, HYSPLIT (Take GZ for example, Figure S1(a)) and FLEXPART-WRF (Figure 6(f)) showed that the air flow was mostly from Southeast Asia at levels over the boundary layer ((Figure 6(f)), and hence had undergone long-range transport. Second, the windspeed near the surface suddenly became very low. Therefore, there had been a rapid change in the windspeed. Based on conservation laws for air mass, it would be expected for there to be some reasonable amount of mixing of the air vertically. This was consistent with the finding that some of the air which has undergone long-range transport would have mixed into the surface region. Furthermore, the ratio of OC to EC concentrations was the minimum measured values on 12th June, with a mean ratio of 1.32 and 2.39 in GZ and ZH, respectively. Also, OC showed a bi-modal distribution, although predominantly in the fine mode while EC mostly peaked at fine mode particles (Take GZ for example, Figure S1 (g-h)), indicating that the organic aerosol was mostly primary, as would be expected from large fire sources. Additionally, the K⁺ concentration on 12th June was about 2-3 times higher than that of mean value measured in GZ and ZH (Take GZ for example, Figure 10(a-b), and Figure S1(i)). Na⁺ and Cl⁻ size distribution were found to be uni-modal distribution in GZ, where they peaked in the 1.0-1.44 μ m size range. Na⁺ and Cl⁻ were bi-modal distribution in ZH on 12th Jun. (figures not showed here). All of these findings above, including the time of the year and the location, are consistent with the long-range transported biomass burning from Southeast Asia (Cohen, 2014).’

Line 485 Is this paragraph saying that MODIS fire hotspots are not useful to see effects of biomass burning?

Response:

We do not state that in general MODIS fire hotspots are not useful. In fact, they have been shown to be very useful in many dry areas and in many temperate and arctic areas. This is why they are commonly used. However, our results show that MODIS fire hotspots are not very useful in wet and tropical regions. This has been published before, such as Cohen, 2014, Giglio et al., 2006 and Yu et al., 2015. MODIS fire hotspots are obstructed by both clouds and high levels of aerosols in the atmosphere, both of which are found associated with tropical forest fires. Additionally, due to the highly wet ground surface, a significant amount of the fires may low temperature and therefore not observable using the MODIS sensors. We make clear this in the text in line 550-555:

‘This result showed that the MODIS fire hotspots are not very useful in wet and tropical regions. MODIS fire hotspots are obstructed by both clouds and high levels of aerosols in the atmosphere, both of which are found associated with tropical forest

fires. Additionally, due to the highly wet ground surface, a significant amount of the fires may have low temperature and therefore not be observable using the MODIS sensors (Cohen, 2014, Giglio et al., 2006; Yu et al., 2015)'

Line 494 The EOF technique may be useful, but it means that it is better than the MODIS fire hotspots discussed in the previous paragraph? What is a specific reason?

Response:

There are some physical and mathematical reasons for this. First of all, observing aerosols is significantly easier and more precise. Since they are measured using variables in the visible and infrared, their measurement is more robust than the hotspot products, which are only in the infrared. There are many articles which show that the aerosol errors are roughly 10% of their total value, whereas for fires, they are significantly higher (Morisette et al., 2005a, 2005b; Levy et al., 2007, 2010; Remer et al., 2007).

From a mathematical sense, we are interested in looking at contributions which are significant. Fire hotspots are effectively point measurements, and as such are not spatially robust. Therefore, it is hard to tell what type of significant impact they have on the atmosphere in general. Given the uncertainties in such precise meteorology, it is highly probable that a point measurement may not convert precisely into an inverse method of atmospheric transport. Whereas AOD is an area measurement, and is a continuous measurement, since the aerosols transport and spread. Therefore, if a significant signal exists, it is far easier to track and transport, at the scale of the inverse meteorological methods used here.

We have added more information in line 558-563:

'Since MODIS fire hotspots are effectively point measurements, and as such are not spatially robust, while AOD are continuous and more easier to be observed, and provides more precise and robust spatial information (Morisette et al., 2005a, 2005b; Levy et al., 2007, 2010; Remer et al., 2005). Therefore, if a significant signal exists, it is far easier to track and transport, at the scale of the inverse meteorological methods used here.'

Figure 2 Please specify which species use the left and right Y-Axes.

Response:

Thanks for the comment. The right Y-Axes was only used for sulfate and the left Y-Axes was for nitrate, ammonium, OC and EC. We have clarified it in line 976-977:

'The mass size distribution of major compositions (SO_4^{2-} , NO_3^- , NH_4^+ , OC and EC) at the three sites during the study period (SO_4^{2-} is plotted against the right Y-Axes)'

Figure 4 Why do these figures look different from other species shown in other

figures? They should be consistent.

Response:

Thanks for the suggestion and we have re-plotted the Figure 5 to make all the figures consistent.

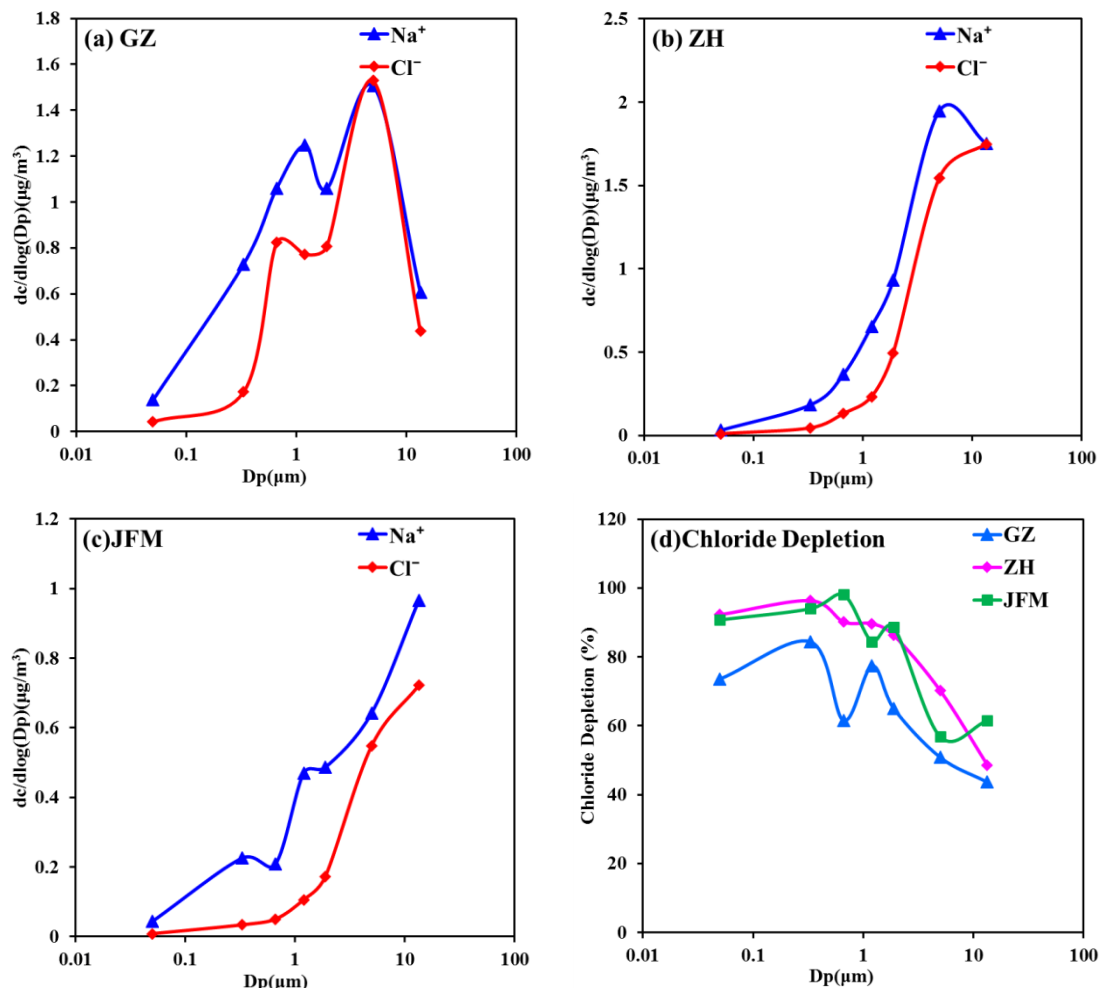


Figure 5. The mass size distribution of (a-c) Na^+ and Cl^- and (d) percentage of chloride depletion at the three sites

Reference:

Heald, C.L. and Spracklen, D.V.: Atmospheric budget of primary biological aerosol particles from fungal spores, *Geophysical Research Letters*, 36, L09806, doi:10.1029/2009GL037493, 2009.

Huang, Z.E., Harrison, R.M., Allen, A.G., James, J.D., Tilling, R.M. and Yin, J.X.: Field intercomparison of filter pack and impactor sampling for aerosol nitrate, ammonium, and sulphate at coastal and inland sites, *Atmospheric Research*, 71, 215-232, doi:10.1016/j.atmosres.2004.05.002, 2004.

Levy, R., Remer, L., and Dubovik, O.: Global aerosol optical properties and application to Moderate Resolution Imaging Spectroradiometer aerosol retrieval over land, *Journal of Geophysical Research*, 112, 1-15, doi:

- 10.1029/2006JD007815, 2007.
- Levy, R., Remer, L., Kleidman, R., et al.: Global evaluation of the Collection 5 MODIS darktarget aerosol products over land, *Atmospheric Chemistry and Physics*, 10, 10399-10420, doi:10.5194/acp-10-10399-2010, 2010.
- Liu, S., Hu, M., Slanina, S., He, L.Y., Niu, Y.W., Brüeggemann, E., Gnauk, T. and Herrmann, H.: Size distribution and source analysis of ionic compositions of aerosols in polluted periods at Xinken in Pearl River Delta (PRD) of China, *Atmospheric Environment*, 42, 6284-6295, doi:http://dx.doi.org/10.1016/j.atmosenv.2007.12.035, 2008.
- Lu, Q., Zheng, J.Y., Ye, S.Q., Shen, X.L., Yuan, Z.B. and Yin, S.S.: Emission trends and source characteristics of SO₂, NO_x, PM₁₀ and VOCs in the Pearl River Delta region from 2000 to 2009, *Atmospheric Environment*, 76, 11-20, doi: http://dx.doi.org/10.1016/j.atmosenv.2012.10.062, 2013.
- Morisette, J.T., Giglio, L., Csiszar, I. and Justice, C.O.: Validation of the MODIS active fire product over Southern Africa with ASTER data, *International Journal of Remote Sensing*, 26, 4239-4264, doi: 10.1080/01431160500113526, 2005a.
- Morisette, J.T., Giglio, L., Csiszar, I., Setzer, A., Schroeder, W., Morton, D. and Justice, C.O.: Validation of MODIS active fire detection products derived from two algorithms, *Earth Interaction*, 9, 1-23, doi: http://dx.doi.org/10.1175/EI141.1, 2005b.
- Remer, L., Kaufman, Y., Tanre, D., Mattoo, S., Chu, D.A., Martins, J.V., Li, R.R., Ichoku, C., Levy, R.C., Kleidman, R.G., Eck, T.F, Vermote, E. and Holben, B.N.: The MODIS Aerosol Algorithms, Products, and Validation, *Journal of Atmospheric Science*, 62, 947-973, doi: 10.1175/JAS3385.1, 2005.
- Stelson, A.W. and Seinfeld, J.H.: Relative humidity and temperature dependence of the ammonium nitrate dissociation constant, *Atmospheric Environment*, 16, 983-992, doi:10.1016/0004-6981(82)90184-6, 1982.
- Wang, Y., Zhuang, G.S., Tang, A.H., Yuan, H., Sun, Y.L., Chen, S. and Zheng, A.H.: The ion chemistry and the source of PM_{2.5} aerosol in Beijing, *Atmospheric Environment*, 39, 3771-3784, doi:10.1016/j.atmosenv.2005.03.013, 2005.
- Yang, X. and Wenig, M.: Study of columnar aerosol size distribution in Hong Kong, *Atmospheric Chemistry and Physics*, 9, 6175-6189, doi:10.5194/acp-9-6175-2009, 2009.
- Yao, X.H., Ling, T.Y., Fang, M. and Chan, C.K.: Comparison of thermodynamic predictions for in situ pH in PM_{2.5}, *Atmospheric Environment*, 40, 2835-2844, doi:10.1016/j.atmosenv.2006.01.006, 2006.
- Yu, C., Chen, L.F., Li, S.S., Tao, J.H. and Su, L.: Estimating Biomass Burned Areas from Multispectral Dataset Detected by Multiple-Satellite, *Spectroscopy and Spectral Analysis*, 35, 739-745, doi:10.3964/j.issn.1000-0593(2015)03-0739-07, 2015.
- Zhang, Z.S., Engling, G., Zhang, L.M., Kawamura, K., Yang, Y.H., Tao, J., Zhang, R.J., Chan, C.Y. and Li, Y.D.: Significant influence of fungi on coarse carbonaceous and potassium aerosols in a tropical rainforest, *Environmental Research Letters*, 10, 034015, doi:10.1088/1748-9326/10/3/034015, 2015.

- Zheng, J.Y., Zhang, L.J., Che, W.W., Zheng, Z.Y. and Yin, S.S.: A highly resolved temporal and spatial air pollutant emission inventory for the Pearl River Delta region, China and its uncertainty assessment, *Atmospheric Environment*, 43, 5112-5122, doi: <http://dx.doi.org/10.1016/j.atmosenv.2009.04.060>, 2009.
- Zhou, S.Z., Davy, P.K., Wang, X.M., Cohen, J.B., Liang, J.Q., Huang, M.J., Fan, Q., Chen, W.H. Chang, M., Ancelet, T. and Trompetter, W.J.: High time-resolved elemental components in fine and coarse particles in the Pearl River Delta region of Southern China: Dynamic variations and effects of meteorology, *Science of the Total Environment*, doi: 10.1016/j.scitotenv.2016.05.194, 2016 (in press).

1 **Properties of aerosols and formation mechanisms**
2 **over southern China during the monsoon season**

3 **Weihua Chen¹, Xuemei Wang^{2*}, Jason Blake Cohen², Shengzhen Zhou^{2*},**
4 **Zhisheng Zhang³, Ming Chang¹, and Chuen Yu Chan⁴**

5 *¹School of Environmental Science and Engineering, Sun Yat-Sen University,*
6 *Guangzhou, China*

7 *²School of Atmospheric Sciences, Sun Yat-Sen University, Guangzhou, China*

8 *³South China Institute of Environmental Sciences, Guangzhou, China*

9 *⁴Key Laboratory of Aerosol, SKLLQG, Institute of Earth Environment, Chinese*
10 *Academy of Sciences, Xi'an, China*

11

12

13 *Corresponding author:
14 Xuemei Wang (eeswxm@mail.sysu.edu.cn)
15 Shengzhen Zhou (zhoushz3@mail.sysu.edu.cn)

16

17 **Abstract**

18 Measurements of size-resolved aerosols from 0.25 to 18 μm were conducted at three
19 sites (urban, suburban and background sites) and used in tandem with an atmospheric
20 transport model to study the size distribution and formation of atmospheric aerosols in
21 southern China during the monsoon season (May-June) in 2010. The mass
22 distribution showed the majority of chemical components were found in the smaller
23 size bins ($<2.5 \mu\text{m}$). Sulfate, was found to be strongly correlated with aerosol water,
24 and anti-correlated with atmospheric SO_2 , hinting at aqueous-phase reactions being
25 the main formation pathway. Nitrate was the only major species that showed a
26 bi-modal distribution at the urban site, and was dominated by the coarse mode in the
27 other two sites, suggesting that an important component of nitrate formation is
28 chloride depletion of sea salt transported from the South China Sea. In addition to
29 these aqueous-phase reactions and interactions with sea salt aerosols, new particle
30 formation, chemical aging, and long-range transport from upwind urban or biomass
31 burning regions were also found to be important in at least some of the sights on some
32 of the days. This work therefore summarizes the different mechanisms that
33 significantly impact the aerosol chemical composition during the Monsoon over
34 southern China.

35 **Keywords:** chemical component, mass size distribution, aqueous-phase reaction
36 chloride depletion

37
38
39
40
41
42
43
44

45 1. Introduction

46 Atmospheric aerosols are solid and liquid substances ubiquitously suspended in
47 the Earth's atmosphere, that impair visibility, negatively affect human health, and
48 directly and indirectly impact regional and global climate (Burnett et al., 2014; Chen
49 et al., 2013a; Chung and Seinfeld, 2005; Cohen et al., 2011; Huang et al., 2014;
50 Jacobson, 2001; Kim et al., 2008; Liu et al., 2011; Ramanathan and Carmichael, 2008;
51 Rosenfeld et al., 2014; Tao et al., 2009). The size distributions and chemical
52 composition of aerosols play essential roles on their transport, transformation,
53 removal mechanisms (Cohen and Prinn, 2011; Cohen and Wang, 2013; Delene and
54 Ogren, 2002; Dubovik et al., 2000; Giglio et al., 2003, 2006; Petrenko, et al., 2012;
55 Seinfeld and Pandis, 2006; Zhao and Gao, 2008a). And also, to some extent, they
56 provide useful information to validate and improve model performance (Cohen and
57 Wang, 2013; Cohen, 2014; Cohen and Lecoecur, 2015; Myhre et al., 2013; Pillai and
58 Moorthy, 2001; Schuster et al., 2006; Tsigaridis et al., 2014). In the environment, the
59 most important aerosol processes occur over the Aitken ($<0.1 \mu\text{m}$), condensation
60 ($\sim 0.1\text{-}0.5 \mu\text{m}$), droplet ($\sim 0.5\text{-}2.0 \mu\text{m}$), and coarse ($>2.0 \mu\text{m}$) size modes (Seinfeld and
61 Pandis, 2006), where new particles are formed in the Aitken mode via condensational
62 growth and coagulation of nucleation mode particles, and droplet mode particles are
63 produced by in-cloud processing or aqueous reactions (Ervens et al., 2011; Lim et al.,
64 2010; Meng and Seinfeld, 1994; Volkamer et al., 2009; Wang et al., 2012; Yao et al.,
65 2003a). On the other hand, coarse mode aerosols usually come from very different
66 sources than smaller aerosols. For example, natural sources such as sea spray, dust,

67 soil, and active biological aerosols are unique and therefore provide further
68 information about the aerosol distribution at a given location.

69 Previous research suggests that sulfate is mostly contained in the non-coarse
70 modes, with the conversion of SO₂ occurring mostly via gas-phase oxidation followed
71 by condensation, or through droplet mode sulfate produced from fog/cloud process
72 (Barth et al., 1992; Meng and Seinfeld, 1994). On the other hand, nitrate usually has a
73 bi-modal distribution with peaks in both the fine and coarse modes. Fine mode nitrate
74 is formed mainly by oxidation of NO₂ to HNO₃ and subsequent condensation, or from
75 the heterogeneous hydrolysis of N₂O₅, while coarse mode nitrate is often observed
76 due to the effect of chloride depletion of sea salt aerosols (Harrison and Pio, 1983;
77 Pierson and Brachaczek, 1998). Ammonium is mostly found in the fine mode and is
78 chemically associated with sulfate and nitrate. Carbonaceous materials, organic
79 carbon (OC) and elemental carbon (EC), are both found primarily in the non-coarse
80 mode. While both OC and EC are impacted by differing emissions sources and wet
81 deposition, there are other significant differences: EC is hydrophobic and radiatively
82 active, while OC is hydrophylic and further has significant source terms from
83 condensation and secondary particle formation (Lan et al., 2011).

84 A series of studies about the mass size distribution of aerosol chemical
85 components have conducted at a specific site over Southern China during the past
86 decade (Lan et al., 2011; Liu et al., 2008; Yang and Wenig, 2009; Zhang et al., 2015).
87 Compared with the previous studies, this paper presents a unique combination of
88 analytical and measurement techniques. We use measurements of chemical properties

89 and size distribution conducted at three different functional sites, coupled with
90 multiple modeling results, and reprocess remote sensing products using statistical
91 methods, all in tandem with each other, which is not commonly found in other studies.
92 Furthermore, we test our approach in Southern China, which is one of the regions of
93 the world with the most complex meteorology, coming under the influence of the
94 Monsoon, with shifting winds from continental and oceanic sources. Additionally, the
95 season tested is a transition period, during which there were significant
96 meteorological contributions from both remote continental sources as well as oceanic
97 sources. On top of this, Southern China has a combination of high temperature and
98 relative humidity, strong radiative flux, and high oxidative capacity, leading to the
99 promotion of significant secondary aerosol formation.

100 In this paper, we present a unique database of the size-different mass distribution
101 of aerosol chemical components during the Monsoon Season over southern China.
102 The data were sampled from a combination of three different sites, one in an urban
103 area, one in a suburban area, and one in a remote area, providing further insights into
104 the characteristics of size distribution in each of these regions, and discussion on the
105 secondary aerosol formation mechanisms, the identification and impacts of
106 long-range transport of biomass and urban sources, and the impacts of mixing sea-salt
107 and urban pollutants on the characteristics of aerosol size distribution.

108

109 **2. Measurements and methodology**

110 **2.1. Description of the sampling sites**

111 The field study was conducted at three sites in southern China (Figure 1), two of
112 which were situated in Guangdong and the other in Hainan. Guangdong is located in a
113 subtropical monsoon climate, primarily influenced by cold and dry air masses from
114 the North in December to February, and warm and wet air masses from the South
115 China Sea in May to August. It has a single annual local rainy season extending from
116 April to September. Hainan is located further to the south, and has year-round warm
117 to hot weather and a distinct rainy season from May to October.

118 The first site (23.12°N, 113.36°E), is located on the rooftop of a building in the
119 South China Institute of Environmental Sciences, Guangzhou (GZ), a mega-city
120 containing more than 13 million people. The site was located about 50m above
121 ground, in an area surrounded by residential and commercial buildings, with the
122 nearest arterial roads located about 200m away. There were no significant industrial
123 emission sources found around the site. This site was chosen since it is highly
124 representative of a typical megacity.

125 The second site was located at (22.34°N, 113.58°E), on the rooftop of the library
126 at Sun Yat-Sen University, in the city of Zhuhai (ZH), a medium sized city of about
127 1.6 million people located in Southern Guangdong adjacent to Macau. The site was
128 located about 60m above the ground, in an area surrounded by mountains on three
129 sides and the estuary where the Pearl River meets the South China Sea about 500m
130 away on the fourth side. There are no significant industrial or major transportation
131 emissions sources nearby. This site was chosen since it is highly representative of a
132 coastal partially urbanized area.

133 The third site was located at Jianfeng Mountain (JFM, 18.74°N, 108.86°E), in a
134 tropical rainforest situated in the Southwest corner of Hainan. This site is distant from
135 the major cities of Hainan province and is further located about 5km away from the
136 coast. JFM is not directly influenced by anthropogenic emissions and is generally
137 regarded as a background site to investigate the long-range transport (Zhang et al.,
138 2013a). This site was chosen both because it is representative of a remote site and
139 because it receives air masses from three different directions: continental East Asia to
140 the North, the South China Sea to the South, and Southeast Asia to the West.

141

142 **2.2 Sampling of aerosol**

143 To attain size-segregated particle samples, a 6-stage High Flow Impactor (MSP)
144 with an airflow rate of 100 L min⁻¹ was employed, with cutoff diameters (D_p) of 18
145 (inlet), 10, 2.5, 1.4, 1.0, 0.44 and 0.25 μm . A total of 10, 8 and 20 sets of
146 size-segregated particle samples were collected in GZ, ZH and JFM, respectively
147 during the periods of May and June in 2010 (shown in Figure 2). A single set of
148 sample collection lasted for approximately 24h in GZ and ZH, and 48h in JFM. Since
149 the aerosol concentration was relatively low in remote JFM site, we extended the
150 sampling time as long as 48h to allow the chemical components to be detected.

151 The mass concentrations of six cations (Na^+ , NH_4^+ , K^+ , Ca^{2+} , Mg^{2+} , and Ca^{2+}) and
152 seven anions (F^- , Cl^- , NO_2^- , Br^- , SO_4^{2-} , NO_3^- and PO_4^-) were analyzed using an ion
153 chromatography (ICS-3000, DIONEX). Thermal Optical Transmittance (TOT)
154 technique was employed to analyze the quartz filter samples to determine the mass

155 concentrations of organic carbon (OC) and elemental carbon (EC) by the use of
156 Sunset Laboratory OCEC Carbon Aerosol Analyzer. Detailed information of the
157 aerosol sampling and in-lab chemical analytical techniques can be found in Zhang et
158 al. (2013a).

159 To be consistent with the background literature (4 modes include Aitken (<0.1
160 μm), condensation ($\sim 0.1\text{-}0.5 \mu\text{m}$), droplet ($\sim 0.5\text{-}2.0 \mu\text{m}$), and coarse ($>2.0 \mu\text{m}$))
161 (Seinfeld and Pandis, 2006), and the constraints of the size bins measured in this study,
162 we implement $2.5 \mu\text{m}$ as the cut-off size to separate fine and coarse particles, and the
163 size bins from $0.44\text{-}1.4 \mu\text{m}$ was defined as droplet particles in this study. Although we
164 were not able to directly measure aerosol water content, given its importance for the
165 study here, we instead estimate the amount by the use of E-AIM model II (Clegg et al.,
166 1998), as it provides the most accurate prediction compared with other models, like
167 ISORROPIA and SCAPE2 (Yao et al., 2006). The input parameters of the E-AIM
168 model II are temperature, relative humidity, strong acidity (H^+), molar concentrations of
169 NH_4^+ , SO_4^{2-} and NO_3^- ions (Clegg et al., 1998). Further, an approximation of the
170 particle strong acidity $[\text{H}^+]_s$ was calculated using Eq. (1):

$$171 \quad [H^+]_s = 2[SO_4^{2-}] + [NO_3^-] - [NH_4^+] \quad (1)$$

172 The calculation of strong acidity would introduce possible errors due to the
173 exclusion of other ions (e.g. K^+ , Na^+ , Cl^-), but which only exerted a minor influence
174 on the estimation of aerosol acidity due to their lower concentration (Yao et al., 2006).

175 **2.3 Meteorological data**

176 Meteorological parameters, including wind speed (WS), wind direction (WD),

177 temperature (T), relative humidity (RH), pressure (P), and precipitation were
178 simultaneously monitored in GZ and JFM sites with a time resolution of 30 minutes.
179 The same meteorological parameters in ZH, as well as the daily low-level cloud cover
180 data at all three sites, were obtained from the China Meteorological Data Sharing
181 Service System (<http://data.cma.cn/site/index.html>).

182

183 **2.4 Remotely sensed measurements**

184 Aerosol optical depth (AOD), fire products including Fire Radiative Power (FRP),
185 and Fire Quality Assurance [QA] data, were obtained from the MODIS sensors
186 aboard both the AQUA and TERRA satellites. Specifically, we obtained the
187 Collection 6, 3km Level 2 swath product for AOD (Remer et al., 2013), and
188 Collection 5.1, 1km Level 2 swath products for FRP and QA (Giglio et al., 2006). **The**
189 **Collection 5.1 active fire products are daily products and have been improved based**
190 **on the previous collection 5.0 products.** All of the data are cloud-screened, with AOD
191 data being computed using different algorithms over land and water, and the fire data
192 using 19 different channels for quality assurance. We only accept values for FRP and
193 Fire Count where the QA is at least 90%.

194

195 **2.5 Atmospheric transport model**

196 **Two Lagrangian particle dispersion models, the Hybrid Single Particle Lagrangian**
197 **Integrated Trajectory (HYSPLIT) (Draxler and Hes, 1998) and FLEXPART coupled**
198 **with The Weather and Research and Forecasting (WRF) model (FLEXPART –WRF)**

199 (Stohl et al., 1998; Brioude et al., 2013) were applied to determine the origin of air
200 masses in this study, Compared with HYSPLIT, FLEXPART can identify the relative
201 importance of source region that affected the receptor visually. HYSPLIT uses single
202 air parcels to compute trajectories with the use of Global Data Assimilation System
203 (GDAS, $1^\circ \times 1^\circ$) as input data. FLEXPART, on the other hand, uses a larger number of
204 air parcels to compute trajectories based on the higher resolution meteorological
205 predictions provided by mesoscale model WRF. The application of FLEXPART –
206 WRF with a novel convective scheme being added improves the dispersion
207 simulations and results in an overall better simulation, especially for finer scale
208 applications (Brioude et al., 2013; Stohl, 1998). In this case, the region was modeled
209 with a spatial resolution of 27×27 km and a temporal resolution of 1 hour.

210 An Eulerian model, WRF/Chem V3.4.1 was used in this study to simulate the fog
211 process. For this model, the target region was modeled at a spatial resolution of
212 3×3 km and a temporal resolution of 1 hour. Detail information about the WRF/Chem
213 model set-up refers to Situ et al. (2013).

214

215 **3. Results and discussion**

216 **3.1. Overall aerosol characteristics**

217 The time series of PM_{18} chemical compositions at the three sites during the
218 sampling period were shown in Figure 2. The average concentration and standard
219 deviation of PM_{18} was 47.8 ± 20.8 , 24.3 ± 12.1 and 8.1 ± 2.7 $\mu\text{g m}^{-3}$ in GZ, ZH and JFM,
220 respectively. The mean and range of PM_{18} in highly urban GZ was both higher and

221 wider than in suburban ZH and rural JFM, with the respective ranges being 23.3~93.7,
222 13.3~35.1, 4.7~14.3 $\mu\text{g m}^{-3}$ in the three sites. Maximum concentration was found both
223 on 12th Jun. in GZ and ZH, while it was on 3rd Jun. in JFM (to be discussed later).

224 Table 1 listed the average concentration of chemical components in the given
225 size-resolved particle ($\text{PM}_{1.0}$, $\text{PM}_{2.5}$ and PM_{10}) and their percentage of PM_{10} at the
226 three sites. In terms of the mass size distribution, the percentage of $\text{PM}_{1.0}$ to PM_{10} was
227 60.2%, 66.3% and 75.0%, and $\text{PM}_{2.5}$ to PM_{10} was 88.0%, 92.6%, 91.7% in GZ, ZH
228 and JFM, respectively. When considered as a whole, it is the smaller sized particles
229 that dominate the aerosol loading at all three of these sites. Looking at the data on a
230 species-by-species level, most of chemical components were concentrated in fine
231 mode particles, which contribute at least 57% to $\text{PM}_{2.5}$. The sole exception is nitrate at
232 ZH and JFM, which were mainly concentrated in the coarse mode with a percentage
233 of above 90%. Overall, the sum of five major chemical components (i.e. sulfate,
234 nitrate, ammonium, OC, and EC) accounted for about 90% of the total mass
235 concentration of detected chemical components across all three sites.

236 Two of the species, sulfate and OC, were found to dominate the particle
237 composition, with concentration of 11.7 ± 5.2 , 8.8 ± 3.2 , $2.2 \pm 1.5 \mu\text{g m}^{-3}$ for sulfate
238 and 7.2 ± 2.7 , 3.0 ± 1.5 , $1.8 \pm 0.8 \mu\text{g m}^{-3}$ for OC in GZ, ZH and JFM, respectively.
239 Sulfate concentration was much higher than that of OC in urban and suburban
240 locations irrespective of particle size, while OC concentration was similar to that of
241 sulfate in fine particles and slightly higher in coarse particles at the remote site. These
242 findings are consistent with the nature of the sources of sulfur from industrial and

243 power plant (Zheng et al., 2009). In addition, shipping source was becoming
244 increasingly vital for SO₂ emission with an increment of 12% per year in this region
245 (Lu et al., 2013; Zhou et al, 2016)

246 Nitrate, mainly formed from the oxidation of NO_x emitted by mobile vehicles
247 and power plants, showed a remarkable difference between urban and background site,
248 ranging from fourteen to thirty times higher in GZ than in the other sites, especially
249 for fine mode nitrate. This is consistent with its more rapid oxidation of its abundant
250 precursor species, especially so in the urban atmosphere (Cohen et al., 2011). In
251 addition, phase equilibrium was another important reason for the discrepancy in urban
252 and background site since nitrate would tend to exist as gas phase while transported to
253 background areas (Seinfeld and Pandis, 2006). A relatively insignificant concentration
254 of NO₃⁻ in ZH and JFM indicated far less anthropogenic emission of the precursor
255 over these two sites.

256 The values of OC and EC in PM_{2.5} were 7.2 ± 2.7 and 3.4 ± 3.2 $\mu\text{g m}^{-3}$ in GZ,
257 3.0 ± 1.5 and 1.5 ± 0.9 $\mu\text{g m}^{-3}$ in ZH. These values were lower than that found in
258 previous studies done in GZ and ZH during the wet season: OC and EC were 13.1 and
259 $4.6 \mu\text{g}\cdot\text{m}^{-3}$ in GZ in 2007, 14.8 and $8.1 \mu\text{g m}^{-3}$ in GZ in 2002, and 5.4 and $1.9 \mu\text{g m}^{-3}$ in
260 ZH in 2002 (Cao et al., 2004; Tao et al., 2009). Furthermore, OC and EC
261 concentrations in JFM were found to be lower than that at other forest sites in China,
262 such as Hengshan: 3.01 and $0.54 \mu\text{g m}^{-3}$ in 2009 (Zhou et al., 2012), Daihai: 8.1 and
263 $1.81 \mu\text{g m}^{-3}$ in 2007 (Han et al., 2008), and Taishan: 6.07 and $1.77 \mu\text{g m}^{-3}$ in 2007
264 (Wang et al., 2011). However, the EC and OC in JFM were similar to some

265 background sites in other countries, such as Puy De Dome in France: 2.4 and 0.26 μg
266 m^{-3} in 2004 (Pio et al., 2007) and Sonnblick in Austria: 1.38 and 0.23 $\mu\text{g m}^{-3}$ in 2003
267 (Pio et al., 2007). This finding is not unexpected, since there are very few urban
268 sources near the site. It is therefore relatively representative of a remote background
269 site, and will be treated as such subsequently in this paper.

270

271 **3.2. Size distribution by chemical composition**

272 The mass size distribution of major compositions at the three sites during the
273 study period, **shows** that sulfate had a single-peaked distribution, with the maximum
274 value found in the 0.44-1.0 μm size over all sites and under all different
275 meteorological conditions examined in this study. The droplet mode sulfate was about
276 $56.0 \pm 8.0 \%$, $63.5 \pm 5.1 \%$ and $58.8 \pm 9.4 \%$ of the total sulfate mass in GZ, ZH and
277 JFM, respectively (Figure 3). This confirms that secondary processing is essential,
278 with aqueous-phase reactions playing a crucial role on the formation and/or growth of
279 droplet sulfate, throughout all of these different regions. It is interesting to note that
280 ZH had the highest relative concentration of droplet mode sulfate, which although it
281 is less urban than GZ, is consistent with the fact that it is located very close to large
282 amounts of sulfur emissions from the shipping traffic at the massive nearby ports of
283 Hong Kong and Shenzhen (Lu et al., 2013).

284 Droplet mode ammonium was mainly due to ammonia vapor that reacted with or
285 condensed on an acidic particle surface. Ammonia was observed to highly correlate
286 with sulfate at the three sites ($R > 0.81$, $P < 0.01$), particularly so in the size range of

287 0.44-1.0 μm . This is consistent with the fact that sulfuric acid preferentially reacts
288 with ammonia (Zhuang et al., 1999), and that most of sulfate in the atmosphere is
289 generally found as ammonium sulfate in the droplet mode (Liu et al., 2008; Zhuang et
290 al., 1999).

291 The nitrate size distribution was found to be bi-modal in GZ, with the peaks
292 occurring in the 0.44-1.0 μm and 2.5-10 μm size ranges. This is consistent with the
293 fact that Droplet mode nitrate was dominated by the heterogeneous aqueous reaction
294 of gaseous nitric acid (HNO_3) and ammonia (NH_3) on the wet surfaces of pre-existing
295 aerosols within ammonia-rich environment, otherwise by heterogeneous hydrolysis of
296 N_2O_5 on the pre-existing aerosols within ammonia-poor conditions. The dissociation
297 equilibrium of NH_4NO_3 highly depends on temperature and humidity (Stelson and
298 Seinfeld, 1982). On the other hand, this result is consistent with the fact that nitrate
299 was found mostly in the coarse mode in ZH and JFM, where it accounted for up to 60%
300 of total particulate mass. A higher relative humidity, consistent with the warm and wet
301 atmosphere over the South China Sea, makes gaseous nitric acid more likely to be
302 absorbed by coarse particles in the atmosphere (Anlauf et al., 2006), resulting in a
303 higher relative concentration of nitrate in the coarse mode in ZH and JFM (where the
304 relative humidity averaged 80 and 91% respectively, as compared to only 73% in GZ).
305 Further, the presence of coarse mode nitrate is consistent with chlorine reduction, as
306 talked about later.

307 OC and EC showed a similar mono-modal distribution in GZ and ZH, with a
308 dominant and a broad peak over the range from 0.25-1.4 μm . On the other hand, a

309 bi-modal distribution was found in JFM. In urban and suburban areas, there are
310 significant primary sources from traffic and industry in the e.g. Huang et al. (2006)
311 and Cao et al. (2004). It is also consistent with the **high-level** emissions due to the
312 ship traffic to Shenzhen and Hong Kong, both of which are located near ZH, which in
313 turn would compensate for the otherwise reduced industrial and traffic sources (**Zheng**
314 **et al., 2012**). OC has both primary sources, which are similar to those for EC as well
315 as secondary formation. There were a few days in which the ratios of OC to EC are
316 not consistent, indicating a large secondary source of OC. We investigated these days
317 and find that **emissions that long-range transported from far-upwind areas with highly**
318 **urbanization or with the existence of biomass burning are responsible, as discussed**
319 **later in this paper**. Additionally, there is some coarse mode OC present in JFM,
320 suggesting a possible source of biological aerosol (**e.g. pollen, spores and plant**
321 **fragment**) (Heald and Spracklen, 2009; Seinfeld and Pandis, 2006; Zhang et al., 2015),
322 which is consistent with the large amounts of vegetation present in that region (**Zhang**
323 **et al., 2015**).

324

325 **3.3. Observed Aqueous-phase reaction of droplet mode sulfate**

326 The daily droplet mode sulfate ranged from 3.0-13.6, 1.6-9.5 and 0.5-4.9 $\mu\text{g m}^{-3}$
327 in GZ, ZH and JFM respectively. **In order to study the aqueous-phase reaction of**
328 **droplet mode sulfate, cases with the air masses came from continent were excluded to**
329 **avoid the effect of transported pollutants on the concentration of sulfate. Then two**
330 **cases with a concentration of droplet sulfate above the mean plus one standard**

331 deviation were selected as typical cases in each site (8th and 12th May in GZ, 12th May
332 and 1st Jun. in ZH, and 4th and 13th May 2010 in JFM), which were more obvious to
333 observe to investigate the effect of aqueous-phase reaction in the formation of droplet
334 mode sulfate (blue shade in Figure 2). In each of these cases, it was found that droplet
335 mode sulfate accounted for about two thirds of the total mass concentration of sulfate
336 at the three sites.

337 A backward trajectory analysis found that during these events, the air masses at
338 these sites mainly originated over the South China Sea (figures not shown here).
339 Additionally, it was determined that during these times at the three sites, there was an
340 abnormally high amount of low cloud cover 60-70% and a relatively higher relative
341 humidity (75~83%) (Table 2). This combination is consistent with moist air being
342 transported over land where the ship and industrial SO₂ emissions can undergo
343 chemistry in the presence of large amounts of liquid cloud water, to form
344 droplet-mode sulfate.

345 We estimated the liquid water content using the AIM-II model (Equation 1). The
346 results showed a significant positive correlation with droplet mode sulfate in GZ
347 (R=0.98, P<0.05), ZH (R=0.53, P<0.05) and JFM (R=0.80, P<0.05), indicating that
348 water content correlated closely with the sulfate aerosol loadings. This is further
349 evidenced that aqueous formation was likely an important contributing factor.

350 We further investigated the aqueous-phase reaction of particles due to the fog
351 process for the data from 8th May in GZ. This is because the measured visibility met
352 the World Meteorological Organization cutoff value of less than 1 km due to water

353 droplets, in the early morning (05:00-07:00 LT) (Figure 4(c)). Consistently, during
354 this time, it was found that the relative humidity was quite high ($RH > 90\%$) and the
355 wind was quite low (wind speeds $< 1.0 \text{ m s}^{-1}$). Also during this time, the cloud fraction
356 and simulated 2m relative humidity were up to 90% over Southern China (Figure
357 4(a-b)). Furthermore, the depression dew point ($\Delta T = T - T_d$, while T_d denotes dew
358 point temperature) was lower than 1 (Figure 4(c)), which indicating that vapor
359 pressure was saturated. An accompanying analysis using WRF/Chem shows that
360 simulated cloud water mixing ratio was the highest during this period over the GZ
361 area and higher value was found around 06:00 LT (Figure 4(e-f)). This combination
362 promoted the existence of fog/low cloud.

363 Further analysis was done by looking at measurements of SO_2 (data from
364 Guangzhou Environmental Protection Bureau, <http://www.gzepb.gov.cn/>). The
365 diurnal variation on 8th May showed a unique pattern compared with the mean diurnal
366 pattern as measured during 2009-2011 (Figure 4(d)). On this day, the SO_2
367 concentration has decreased dramatically since 05:00-07:00 LT, which is consistent
368 with SO_2 transferred from the gas to aqueous phase due to the high solubility of SO_2
369 in fog water droplets (Zhang et al., 2013b).

370 Simulation of these conditions using WRF/Chem indicates that the rapid growth
371 of both Aitken and accumulation ($\sim 0.1\text{-}1 \mu\text{m}$) mode sulfate started at 07:00 LT and
372 peaked at 08:00-09:00 LT (Figure 4(g-h)). This further supports the conclusion of
373 fresh sulfate production, in this case through both the aqueous and potential initial gas
374 to particle formation, followed by condensation/coagulation and uptake into the liquid

375 droplets present. All of this is consistent with generalized urban modeling studies
376 performed under similar conditions (e.g. Cohen and Prinn, 2011).

377

378 **3.4. Observed interactions between nitrate and chloride depletion**

379 The mass size distribution of Cl^- and Na^+ showed a similar pattern to nitrate at the
380 three sites, peaking in coarse mode particles (Figure 5(a-c)) with an average
381 percentage of 43%, 62% and 43% for coarse mode Na^+ , 53%, 76% and 74% for
382 coarse mode Cl^- in GZ, ZH and JFM, respectively, suggesting the main sea salt
383 sources. Na^+ and Cl^- shown a bi-modal distribution in GZ, illustrating the combustion
384 emissions, e.g. biomass burning or coal combustion for fine mode Na^+ and Cl^- (Wang
385 et al., 2005), but the contributions were insignificant since the magnitude of Na^+ and
386 Cl^- from combustion sources is many orders of magnitude smaller than oceanic
387 sources. Furthermore, if the biomass burning source were significant, it would clearly
388 also show up in terms of the K^+ and BC/OC ratio, as explained later in the section 3.6

389 *Quantifying the impacts of fires.*

390 The concentration and percentage of chloride depletion ($[\text{Cl}_{dep}]$ and $\% \text{Cl}_{dep}$)
391 were calculated using Eq. (2-3), where $[\text{Cl}_{meas}^-]$ and $[\text{Na}_{meas}^+]$ are the measured molar
392 concentrations of chloride and sodium respectively, 1.174 was the molar ratio of Cl^- to
393 Na^+ in sea water (Yao et al., 2003b).

$$394 \quad [\text{Cl}_{dep}] = 1.174[\text{Na}_{meas}^+] - [\text{Cl}_{meas}^-] \quad (2)$$

$$395 \quad \% \text{Cl}_{dep} = \frac{1.174[\text{Na}_{meas}^+] - [\text{Cl}_{meas}^-]}{1.174[\text{Na}_{meas}^+]} * 100\% \quad (3)$$

396 The positive value of $[\text{Cl}_{dep}]$ represents chloride depletion, otherwise means the

397 chloride enrichment, suggesting additional sources was existed for Cl^- excluding sea
398 salt. Therefore, samples with negative $[\text{Cl}_{dep}]$ were excluded from analysis to avoid
399 the effect of non-sea salt emission on chloride depletion.

400 In general, the $\% \text{Cl}_{dep}$ decreased as the aerosol mass increased (Figure 5(d)).
401 Chloride had been almost entirely depleted in fine mode particles with the value of
402 91%, while the value was 60% in coarse mode particles in ZH and JFM. The chloride
403 depletion was relatively weaker in GZ with a value of 72% and 47% in fine and
404 coarse mode particle, which was in consistent with that the urban area was less
405 affected by ocean emission. The result was consistent with a study conducted in South
406 China Sea in 2004 as well as the theory that reaction between sulfuric acid and nitric
407 acid with sea salt (sodium chloride) is facilitated in fine particles due to their larger
408 surface areas to volume ratio and longer atmospheric residence time (Chatterjee et al.,
409 2010; Hsu et al., 2007).

410 The ratio of calculated ammonium to measured ammonium was used to explain
411 the presence of sulfuric acid and nitric acid in the aerosol, with a value larger than 1
412 indicating there was insufficient ammonium to neutralize nitric acidic NO_3^- (since
413 ammonium first consumes sulfuric acid). Calculated ammonium was equal to
414 $2 * [\text{nss-SO}_4^{2-}] + [\text{NO}_3^-]$, where $[\text{nss-SO}_4^{2-}]$ and $[\text{NO}_3^-]$ represents the molar concentration
415 of non-sea-salt SO_4^{2-} (i.e., $[\text{nss-SO}_4^{2-}] = [\text{SO}_4^{2-}] - 0.14 * [\text{Cl}^-]$) and NO_3^- (Huang et al.,
416 2004). The calculated ratio was much higher than 1 in ZH and JFM suggesting that
417 nitrate plays a role in Cl depletion. The ratio of nitrate to percent chloride depletion
418 can then be used to calculate the contribution of coarse nitrate to chloride depletion

419 (Zhuang et al., 1999; Zhao and Gao, 2008b). This result showed that nitrate was
420 responsible for the depletion of 54% and 17% of coarse chloride in ZH and JFM
421 respectively. This suggests that the interaction of sea salt particles with anthropogenic
422 pollutants is an important pathway for the generation of aerosol species in coastal
423 suburban regions like ZH, which have sizable amounts of both sea salt and NO_x
424 emissions (Chatterjee et al., 2010; Liu et al., 2008).

425 Relative humidity exceeded 80% during the whole sampling time in ZH except
426 for 24th May, which was 64% and the air mass mainly came from northern
427 continental areas. The only other day that had a significant continental wind source at
428 ZH with a higher relative humidity (80%) was found on 7th June. The percentage of
429 chloride depletion was 95% and 69% for fine and coarse particles on 24th May and the
430 value was 78% and 64% on 7th Jun. There was no distinct difference found in coarse
431 particles for the two cases, there was a considerable difference in fine particles with
432 higher chloride depletion happened on 24th May. The meteorological conditions were
433 similar on these two days excluding humidity, moreover, the aerosol water content in
434 fine mode particles was about 8 times higher on 7th Jun. ($3.6 \mu\text{g m}^{-3}$) than that on 24th
435 May ($0.45 \mu\text{g m}^{-3}$). This finding suggested that humidity or aerosol water content
436 would be an important factor that affected the chloride depletion, which is consistent
437 with our understanding of the release of hydrochloric acid under the known high nitric
438 acid conditions, especially when there is less aerosol water (at relatively lower
439 humidity) to dissolve all of the volatiles, which would shift HNO₃ from gas- to
440 particle-phase and further to reinforce the release of hydrochloric acid (Chen et al.,

441 2013b; Dasgupta et al., 2007). In addition, the concentration of coarse mode nitrate
442 was similar for these two days with a value of 1.3~1.4 $\mu\text{g m}^{-3}$, but the concentration of
443 fine mode nitrate was about 4 times higher on 24th May (0.18 $\mu\text{g m}^{-3}$) than that on 7th
444 Jun. (0.04 $\mu\text{g m}^{-3}$), further suggesting the relative lower humidity favor the particle
445 phase nitrate over chloride.

446

447 3.5. The effects of long-range transport, and in-situ chemistry

448 There were four days that the amounts and properties of the aerosols were
449 significantly impacted by long range transport and unique formation and alteration
450 mechanisms: one in each GZ and ZH (both occurring on 12th June) and three in JFM
451 (1st, 3rd, and 5th June).

452 On 12th June in both GZ and ZH, the total aerosol concentration was the highest
453 measured, at respectively 93.7 and 35.1 $\mu\text{g}\cdot\text{m}^{-3}$ in GZ and ZH (Figure 2). Secondly,
454 the concentration of secondary soluble ions was the highest measured. The Sulfur
455 Oxidation Ratio (SOR) and Nitrogen Oxidation Ratio (NOR) are applied to indicate
456 the degree of oxidation of SO_2 and NO_2 precursor gases (Wang *et al.*, 2005). The
457 equations for SOR and NOR are calculated as $\text{SOR} = n\text{-SO}_4^{2-} / (n\text{-SO}_4^{2-} + n\text{-SO}_2)$ and
458 $\text{NOR} = n\text{-NO}_3^- / (n\text{-NO}_3^- + n\text{-NO}_2)$, where $n\text{-SO}_4^{2-}$ and $n\text{-NO}_3^-$ are the molar concentrations
459 of particulate SO_4^{2-} and NO_3^- and $n\text{-SO}_2$ and $n\text{-NO}_2$ are the molar concentrations of
460 the precursor gases SO_2 and NO_2 . SOR and NOR was also the highest On 12th June at
461 the range of 0.44-1.0 μm in GZ with the value of 0.20 and 0.17, respectively (Figure 6
462 (a-b)) (no supported data to estimate SOR and NOR in ZH on this day). Thirdly, this

463 was the only day in GZ that the nitrate size distribution was found to be uni-modal,
464 where it peaked in the 1.0-1.44 μm size range (Figure 6 (d)), which was the largest of
465 any mean size nitrate in GZ measured. Meanwhile, the nitrate size distribution
466 changed from coarse mode to bi-modal and peaked in 0.25-0.44 μm size range in ZH
467 measured on this day (Figure S1(j)). Fourthly, the peak of sulfate and ammonia
468 shifted from typical values in the 0.44-1.0 μm size range to the 1.0-1.44 μm size range
469 (Take GZ for example, Figure 6(c) and Figure S1(f)). All of these are consistent with
470 enhanced secondary production. Such a statistically enhanced amount of secondary
471 production requires the aerosols to have had considerably more time in the
472 atmosphere to have aged as they have, and therefore is consistent with them having
473 undergone considerable long range transport (Cohen et al., 2011).

474 To provide further evidence, 3-day air mass backward trajectories were conducted
475 at each of the three sites. The parcels were released at initial heights of 100, 500,
476 1000 and 2000m, hourly, as a means of robustly sampling the boundary layer
477 throughout the day. The results showed that air masses winded up over GZ and ZH
478 in the lower free troposphere or near the top of the boundary layer had mostly
479 originated over continental Southeast Asia, while those winding up near the surface,
480 had mostly come from Northern China (Take GZ for example, Figure S1(a)).
481 Furthermore, since the air masses came from opposite directions at nearly the same
482 time, the end result was observed to be a stable meteorological condition over GZ
483 (very low wind 0.1 m s^{-1}) and ZH (wind speed was 1m/s which was the lowest
484 during the sampling times). In fact, it seems from the back trajectory analysis that

485 there was descending air in and around GZ and ZH on this day, which implies that
486 air transported from far away in the lower free-troposphere would have been
487 transported back near the surface (Take GZ for example, Figure S1 (b-c)).
488 FLEXPART-WRF was next applied to address the issue of the air residence time
489 through the column over GZ and ZH for that day. Take GZ for example, as can be
490 shown in Figure 6 (e-f), there was a strong influence from the local region of GZ and
491 surrounding adjoining cities, at a lower altitude (500m and lower) (Figure 6(e) and
492 Figure S1 (d-e)). All of these results were further consistent with the high levels of
493 aerosols measured as well as additional secondary processing having had time to
494 occur.

495 Except for in-situ formation, long-range transport was another impact factor. First,
496 HYSPLIT (Take GZ for example, Figure S1(a)) and FLEXPART-WRF (Figure 6(f))
497 showed that the air flow was mostly from Southeast Asia at levels over the boundary
498 layer ((Figure 6(f)), and hence had undergone long-range transport. Second, the
499 windspeed near the surface suddenly became very low. Therefore, there had been a
500 rapid change in the windspeed. Based on conservation laws for air mass, it would be
501 expected for there to be some reasonable amount of mixing of the air vertically. This
502 was consistent with the finding that some of the air which has undergone long-range
503 transport would have mixed into the surface region. Furthermore, the ratio of OC to
504 EC concentrations was the minimum measured values on 12th June, with a mean
505 ratio of 1.32 and 2.39 in GZ and ZH, respectively. Also, OC showed a bi-modal
506 distribution, although predominantly in the fine mode while EC mostly peaked at

507 fine mode particles (Take GZ for example, Figure S1 (g-h)), indicating that the
508 organic aerosol was mostly primary, as would be expected from large fire sources.
509 Additionally, the K^+ concentration on 12th June was about 2-3 times higher than that
510 of mean value measured in GZ and ZH (Take GZ for example, Figure 10(a-b), and
511 Figure S1(i)). Na^+ and Cl^- size distribution were found to be uni-modal distribution
512 in GZ, where they peaked in the 1.0-1.44 μm size range. Na^+ and Cl^- were bi-modal
513 distribution in ZH on 12th Jun. (figures not showed here). All of these findings above,
514 including the time of the year and the location, are consistent with the long-range
515 transported biomass burning from Southeast Asia (Cohen, 2014).

516 At JFM the total aerosol concentration was highest on the 1st, 3rd, and 5th June. In
517 particular, the levels of EC and potassium were elevated on all three days, and the
518 ratio of OC to EC was depressed (Figure S2 (c-e)). However, in addition to these
519 clues, there were some differences: the levels of sulfate and ammonia were
520 remarkably elevated on the 3rd and 5th June (Figure 7(g) and Figure S2 (b)), likely due
521 to a mixing of urban sources with the fire sources. On the other hand, on the 1st June,
522 the sulfate was lower, but the nitrate was considerably higher, peaking in the coarse
523 mode (Figure 7 (h)), likely due to mixing of South China Sea air with the fire sources.

524 HYSPLIT results showed that on all three of these days, the great majority of air
525 masses arriving at JFM originated from continental Southeast Asia (Figure S2(a)).
526 However, all of these parcels of air arrived in the upper boundary layer or the lower
527 free troposphere. By analyzing the FLEXPART-WRF runs at higher resolution, it was
528 demonstrated that there was a strong influence of air from ocean on 1st June (Figure 7

529 (a-b)) at the lower parts of the boundary layer. This is consistent with the observed
530 non-elevated sulfate and elevated coarse nitrate on that day. Furthermore, the
531 FLEXPART-WRF runs at higher resolution demonstrated a considerable influence of
532 air from Southern China (urban and semi-urban Guangdong Province, including many
533 major shipping lanes) on the 3rd and 5th June, again in the lower parts of the boundary
534 layer (Figure 7(c-f)). This is again consistent with the observed elevated levels of
535 sulfate, due to the in-situ processing of urban emissions as the air was transported to
536 JFM, and then mixing with the fire emissions transported from the other direction at
537 height. Additionally, there was some amount of fine mode nitrate found on the 3rd Jun.,
538 further consistent with the in-situ processing of NO₂ emitted along with biomass
539 combustion, and therefore further evidence that mixing occurred between the two
540 different source regions.

541

542 **3.6. Quantifying the impacts of fires**

543 Taking a first look at the possibility that fires are responsible, as described above,
544 we look at a summary of the statistics of the MODIS Fire Hotspots (Figure 8). As we
545 observe, while the total number of fire hotspots occurring throughout Southeast Asia
546 is moderate in early May, the number reduces to the extent that there are effectively
547 almost no burning parcels. Furthermore, those few square kilometers that are burning
548 are of low radiative intensity, under 200W/m², and hence only moderately or lowly
549 emitting, with the exception of a single day in late June, after the period of interest
550 has ended. **This result showed that the MODIS fire hotspots are not very useful in wet**

551 and tropical regions. Since MODIS fire hotspots are obstructed by both clouds and
552 high levels of aerosols in the atmosphere, both of which are found associated with
553 tropical forest fires. Additionally, due to the highly wet ground surface, a significant
554 amount of the fires may low temperature and therefore not observable using the
555 MODIS sensors (Cohen, 2014, Giglio et al., 2006; Yu et al., 2015).

556 Instead, we follow the approach of Cohen (2014) and look at the once to twice
557 daily measured AOD data (Figure 9), in the context of the Empirical Orthogonal
558 Functions approach (EOF). Since MODIS fire hotspots are effectively point
559 measurements, and as such are not spatially robust, while AOD are continuous and
560 more easier to be observed, and provides more precise and robust spatial information
561 (Morissette et al., 2005a, 2005b; Levy et al., 2007, 2010; Remer et al., 2005).
562 Therefore, if a significant signal exists, it is far easier to track and transport, at the
563 scale of the inverse meteorological methods used here. The rationale is that over
564 Southeast Asia there are only a few known large urban centers (Hanoi, Ho Chi Minh
565 City, and Bangkok). Therefore, any other significant contribution to the variance of
566 measured AOD must be from fires. The EOF technique has been shown to be an
567 optimal manner by which to reproduce both the spatial extent and magnitude of the
568 smoke over Continental Southeast Asia (Cohen, 2014; Cohen and Leocure, 2015).

569 As observed, the major regions of high AOD (average AOD > 0.4) are found over
570 Southeast Asia as described above, with most of the sources coming from fires found
571 in two arcs: one from Eastern Thailand, through Laos, and ending in Central Vietnam;
572 and the other in the forests of Myanmar. The region around Hanoi is hard to decipher,

573 as it could be an urban expansion or fire. Additionally, there are regions found in
574 urban East Asia, including the region between Hong Kong and Guangzhou and
575 urbanization along the Yangtze River, however, all of these are known regions of
576 urbanization and are not regions where fire is important.

577 An EOF Analysis concludes that in fact these are the only two statistically
578 significant EOFs (Figure 10). The measured AOD over both of these regions is clearly
579 elevated compared with the region as a whole throughout the entire time. Furthermore,
580 there is an especially large contribution from these two EOFs compared with the
581 background over Southeast Asia only (excluding AOD measured over China, which is
582 downwind and hence not a fire source region) from May 31st to June 6th. Given the
583 rapid transport time from Southeast Asia to JFM, the fact that these peaks occur
584 within 1 day of the peaks in the fires is reasonable. Additionally, while the overall
585 Southeast Asian AOD drops from the 8th onwards, there is a very significant
586 difference (difference in AOD more than 0.5) between the overall AOD and that over
587 the two source regions again from June 8th to June 13th. Given that there are markers
588 of fires in GZ and ZH on June 12th, including high potassium and a low OC/EC ratio,
589 and that a significant portion of the airflow over these regions originated from
590 Southeast Asia within the past 72 hours, these results are consistent with high fires
591 originating from Southeast Asia, then being transported over the next 72 hours to GZ
592 and ZH. The fact that only one day has such measured conditions at the surface is
593 likely due to the fact that the smoke is mostly concentrated near the boundary layer
594 and hence local vertical mixing was most prevalent on or around June 12th.

595

596 **4. Conclusion**

597 Aerosol samples were collected at three sites using a 6-stage sampler during the
598 local wet season in Southern China (May – Jun.) in 2010, to jointly study the mass
599 and size distributions of aerosol chemical components. **These site observations,**
600 **together with model simulations and remote-sensing data, were used to investigate**
601 **impacts of chemistry and atmospheric transport** on the aerosol formation mechanisms
602 at the three sites over Southern China. These were chosen such that they spanned
603 different source and meteorological regions, at urban site GZ, a suburban site ZH, and
604 a remote and forested site at JFM.

605 Sulfate and Ammonium were found to have a single peaked distribution from
606 0.44-1.0 μ m at all sites over the entire sampling period in this study, and accounted for
607 57.5-99 % of the daily-average total aerosol mass. Aqueous-phase reactions were
608 found to be an essential factor to the formation of droplet sulfate. In addition, we
609 found significant secondary processing and enhancement due to meteorological
610 drivers which were wetter or allowed for a longer residence time.

611 A bi-modal distribution was found for nitrate, with a droplet mode in 0.44-1.0 μ m,
612 indicating that it was formed under heavily polluted conditions or through similar
613 secondary aerosol processing. On the other hand, nitrate had a significant fraction in
614 the coarse mode in ZH and JFM during the wet season, where it accounted for about
615 40% of total mass. In this case, we found that the mass size distribution of nitrate was
616 likely attributed to chloride depletion, with almost complete chloride depletion found

617 in ZH and JFM during the wet season. Additionally, relative humidity was an
618 important consideration in chloride depletion under relatively lower relative humidity,
619 conditions, leading to the increase of coarse mode nitrate.

620 OC and EC showed a broad peak at 0.25-1.0 μ m in GZ and ZH, consistent with
621 significant local sources, from urbanization, transport, residential, and shipping
622 sources. Furthermore, under less heavily polluted conditions, OC was found to have a
623 bi-modal distribution in JFM, with important contributions from secondary particle
624 formation in the fine mode and potential biological aerosol in the coarse mode
625 particles.

626 Additionally, OC and EC were shown to have broad peaks, and a significantly
627 different ratio, raising the likelihood of a mixing of the local emissions with emissions
628 transported long-range from biomass burning in Southeast Asia. These conditions
629 were further supported by a large amount of potassium found jointly with the aerosol.
630 An in-depth analysis of the meteorology, and remotely sensed Fire and AOD
631 properties, in conjunction with a variance maximizing technique, provided further
632 evidence to help us validate this assumption. It is clear that there was a significant
633 impact on GZ and ZH from fire sources from Thailand, Laos, and Vietnam, as well as
634 possible long-range transport of urban emissions from the urban megacity of Hanoi in
635 Vietnam. The combination of local formation and long-range transport played a
636 significant role on the variation of particle chemical compositions.

637 Overall, we found that the size distribution and formation of aerosols greatly
638 depend on emissions, location, and in-situ processing, especially aqueous-phase

639 reactions. Strong local formation and long-range-transport of both urban pollution
640 from GZ and of biomass burning from Southeast Asia all were observed to influence
641 the size distribution of chemical components across all of the area studies. On the
642 other hand, the interaction between sea salt aerosols and anthropogenic pollutants
643 showed significant effects at coastal locations and play an important role in the
644 deterioration of the air quality in Southern China under high relative humidity
645 conditions during the wet season.

646

647 **Acknowledgments**

648 This work was supported by National Science Fund for Outstanding Young Scholars
649 (41425020), China Special Fund for Meteorological Research in the Public Interest
650 (GYHY201406031), National Science & Technology Pillar Program
651 (2014BAC21B02) and Specialized Research Fund for the Doctoral Program of
652 Higher Education in China (2013380004115009). The authors would especially like
653 to thank Prof. Guenter Engling at National Tsing Hua University for helping to
654 chemical analysis at the laboratory.

655

656 **References**

657 Anlauf, K., Li, S.M., Leitch, R., Brook, J., Hayden, K., Toom-Saunty D., and Wiebe,
658 A.: Ionic composition and size characteristics of particles in the Lower Fraser
659 Valley: Pacific 2001 field study, *Atmospheric Environment*, 40, 2662- 2675, doi:
660 10.1016 /j.atmosenv. 2005.12.027, 2006.

661 Barth, M.C., Hegg, D.A., and Hobbs, P.V.: Numerical modeling of cloud and
662 precipitation chemistry associated with two rainbands and some comparisons with
663 observations, *Journal of Geophysical Research*, 97, 5825- 5845, doi:
664 10.1029/92JD00464, 1992.

665 Brioude, J., Arnold, D., Stohl, A., Gassiani, M., Morton, D., Seibert, P., Angevine, W.,
666 Evan, S., Dingwell, A., Fast, J.D., Easter, R.C., Pisso, I., Burkhardt, J., and
667 Wotawo, G.: The Lagrangian particle dispersion model FLEXPART-WRF
668 version 3.1, *Geoscientific Model Development*, 6, 1889-1904, doi: 10.5194/
669 gmd-6-1889-2013, 2013.

670 Burnett, R.T., et al.: An integrated risk function for estimating the global burden of
671 disease attributable to ambient fine particulate matter exposure, *Environmental*
672 *Health Perspectives*, 122, 397, doi:10.1289/ehp.1307049, 2014.

673 Cao, J.J., Lee, S.C., Ho, K.F., Zou, S.C., Fung, K., Li, Y., Watson, J.G., and Chow, J.
674 C.: Spatial and seasonal variations of atmospheric organic carbon and elemental
675 carbon in Pearl River Delta Region, China, *Atmospheric Environment*, 38, 4447–
676 4456, doi:10.1016/j.atmosenv.2004.05.016, 2004.

677 Chatterjee, A., Adak, A., Singh, A.K., Srivastava, M.K., Ghosh, S.K., Tiwari, S.,
678 Devara, P.C.S., and Raha, S.: Aerosol chemistry over a high altitude station at
679 northeastern Himalayas, India, *PLoS ONE*, 5, e11122, doi: 10.1371/journal.
680 pone.0011122, 2010.

681 Chen, S.Y., Huang, J.P., Zhao, C., Qian, Y., Leung, L.R. and Yang, B.: Modeling the
682 transport and radiative forcing of Taklimakan dust over the Tibetan Plateau: A

683 case study in the summer of 2006, *Journal of Geophysical Research*, 118, 797–
684 812, doi:10.1002/jgrd.50122, 2013a.

685 Chen, H.Z., Wu, D., Liao, B.T., Mao, X., Zhuang, H.B., Li, L., Liu, A.M., Li, H.Y.,
686 and Li, F.: Influence of different acidic gases and relative humidity on the chlorine
687 loss of marine aerosols, *Acta Scientiae Circustantiae*, 33, 1141-1149, 2013b (in
688 Chinese with English Abstract).

689 Clegg, S.L., Brimblecombe, P., and Wexler, A.S.: Thermodynamic Model of the
690 System $\text{H}^+ - \text{NH}_4^+ - \text{SO}_4^{2-} - \text{NO}_3^- - \text{H}_2\text{O}$ at Tropospheric Temperatures, *The Journal*
691 *of Physical Chemistry A*, 102, 2137-2154, doi: 10.1021/jp973042r, 1998.

692 Cohen J.B., and Lecoecur, E.: Decadal-scale relationship between measurements of
693 aerosols, land-use change, and fire over Southeast Asia, *Atmospheric Chemistry*
694 *and Physics Discussion*, 15, 26895-26957, doi:10.5194/acpd-15-26895-2015,
695 2015.

696 Cohen, J. B.: Quantifying the Occurrence and Magnitude of the Southeast Asian Fire
697 Climatology, *Environmental Research Letter*, 9, 114018, doi:10.1088/1748-9326/
698 9/11/114018, 2014.

699 Cohen, J. B., and Wang, C.: An Estimate of Global Black Carbon Emissions Using a
700 Top-Down Kalman Filter Approach, *Journal of Geophysical Research* , 119, 1-17,
701 doi:10.1002/2013JD019912, 2013.

702 Cohen, J. B., and Prinn, R.G.: Development of a fast, urban chemistry metamodel for
703 inclusion in global models, *Atmospheric Chemistry and Physics*, 11, 7629-7656,
704 doi:10.5194/acp-11-7629-2011, 2011.

705 Cohen, J. B., Prinn, R.G., and Wang, C.: The Impact of detailed urban-scale
706 processing on the composition, distribution, and radiative forcing of
707 anthropogenic aerosols, *Geophysical Research Letters*, 38, L10808,
708 doi:10.1029/2011GL047417, 2011.

709 Chung S.H., and Seinfeld, J.H.: Climate response of direct radiative forcing of
710 anthropogenic black carbon, *Journal of Geophysical Research*, 110, D11102, doi:
711 10.1029/2004JD005441, 2005.

712 Dasgupta, P.K., Campbell, S.W., Al-Horr, R.S., Ullah, S.M.R., Li, J.Z., Amalfitano, C.,
713 and Poor, N.D.: Conversion of sea salt aerosol to NaNO_3 and the production of
714 HCl: Analysis of temporal behavior of aerosol chloride/nitrate and gaseous
715 HCl/ HNO_3 concentrations with AIM, *Atmospheric Environment*, 41, 4242-4257,
716 doi:10.1016/j.atmosenv.2006.09.054, 2007.

717 Delene, D.J. and Ogren, J.A.: Variability of aerosol optical properties at four North
718 American surface monitoring sites, *Journal of the Atmospheric Sciences*, 59,
719 1135-1150, doi: [http://dx.doi.org/10.1175/1520-0469\(2002\)059](http://dx.doi.org/10.1175/1520-0469(2002)059<1135:VOAOPA>) <1135:VOAOPA>
720 2.0.CO;2, 2002.

721 Draxler, R.R., and Hess, G.D.: An overview of the HYSPLIT_4 modeling system of
722 trajectories, dispersion, and deposition, *Australian Meteorological Magazine*, 47,
723 295-308, 1998.

724 Dubovik, O., Smirnov, A., Holben, B.N., King, M.D., Kaufman, Y.J., Eck, T.F., and
725 Slutsker, I.: Accuracy assessments of aerosol optical properties retrieved from
726 Aerosol Robotic Network (AERONET) Sun and sky radiance measurements,

727 Journal of Geophysical Research, 105, 9791-9806, doi: 10.1029/2000JD900040,
728 2000.

729 Ervens, B., Turpin, B.J., and Weber, R.J.: Secondary organic aerosol formation in
730 cloud droplets and aqueous particles (aqSOA): a review of laboratory, field and
731 model studies, Atmospheric Chemistry and Physics, 11, 11069-11102,
732 doi:10.5194/acp-11-11069-2011, 2011.

733 Giglio, L., Csiszar, I., and Justice, C.O.: Global distribution and seasonality of active
734 fires as observed with the Terra and Aqua Moderate Resolution Imaging
735 Spectroradiometer (MODIS) sensors, Journal of Geophysical Research, 111,
736 G02016, doi: 10.1029 / 2005JG000142, 2006.

737 Giglio, L., Kendall, J.D., and Mack, R.: A multi-year active fire data set for the tropics
738 derived from the TRMM VIRS, International Journal of Remote Sensing, 24,
739 4505- 4525, doi: 10.1080/0143116031000070283, 2003.

740 Han, Y., Han, Z., Cao, J.J., Chow, J.C., Watson, J.G., An, Z.S., Liu, S.X., and Zhang,
741 R.J.: Distribution and origin of carbonaceous aerosol over a rural high-mountain
742 lake area, Northern China and its transport significance, Atmospheric
743 Environment, 42, 2405-2414, doi:10.1016/j.atmosenv.2007.12.020, 2008.

744 Harrison, R.M., and Pio, C.A.: Size differentiated composition of inorganic
745 atmospheric aerosols of both marine and polluted continental origin, Atmospheric
746 Environment, 17, 1733-1738, doi:10.1016/0004-6981(83)90180-4, 1983.

747 Heald, C.L. and Spracklen, D.V.: Atmospheric budget of primary biological aerosol
748 particles from fungal spores, Geophysical Research Letters, 36, L09806, doi:

749 [10.1029/2009GL037493](https://doi.org/10.1029/2009GL037493), 2009.

750 Huang, J.P., Wang, T.H., Wang, W.C., Li, Z.Q. and Yan, H.R.: Climate effects of dust
751 aerosols over East Asian arid and semiarid regions, *Journal of Geophysical*
752 *Research*, 119, 11398–11416, doi: 10.1002/2014JD021796, 2014.

753 Huang, X.F., Yu, J.Z., He, L.Y., and Hu. M.: Size distribution characteristics of
754 elemental carbon emitted from Chinese vehicles: results of a tunnel study and
755 atmospheric implications, *Environmental Science & Technology*, 44, 5355–5360,
756 doi: 10. 1021 /es0607281, 2006.

757 [Huang, Z.E., Harrison, R.M., Allen, A.G., James, J.D., Tilling, R.M. and Yin, J.X.:](https://doi.org/10.1016/j.atmosres.2004.05.002)
758 [Field intercomparison of filter pack and impactor sampling for aerosol nitrate,](https://doi.org/10.1016/j.atmosres.2004.05.002)
759 [ammonium, and sulphate at coastal and inland sites, *Atmospheric Research*, 71,](https://doi.org/10.1016/j.atmosres.2004.05.002)
760 [215-232, doi:10.1016/j.atmosres.2004.05.002, 2004.](https://doi.org/10.1016/j.atmosres.2004.05.002)

761 Hsu, S.C., Liu, S.C., Kao, S.J., Jeng, W.L., Huang, Y.T., Tseng, C.M., Tsai, F.J., Tu,
762 J.Y., and Yang, Y.: Water-soluble species in the marine aerosol from the northern
763 South China Sea: High chloride depletion related to air pollution, *Journal of*
764 *Geophysical Research*, 112, D19304, doi:10.1029/2007JD008844,2007.

765 Kim, S.W., Berthier, S., Raut, J.C., Chazette, P., Dulac, F., and Yoon, S.C.: Validation
766 of aerosol and cloud layer structures from the space-borne lidar CALIOP using a
767 ground-based lidar in Seoul, Korea, *Atmospheric Chemistry and Physics*, 8,
768 3705-3720, doi:10.5194/acp-8-3705-2008, 2008.

769 Jacobson, M.Z.: Global direct radiative forcing due to multicomponent
770 anthropogenic and natural aerosols, *Journal of Geophysical Research*, 106,

771 1551-156, doi: 10.1029/2000JD900514, 2001.

772 Lan, Z.J., Chen, D.L., Li, X., Huang, X.F., He, L.Y., Deng, Y.G., Feng, N., and Hu, M.:
773 Modal characteristics of carbonaceous aerosol size distribution in an urban
774 atmosphere of South China, *Atmospheric Research*, 100, 51-60,
775 doi:10.1016/j.atmosres.2010.12.022, 2011.

776 Levy, R., Remer, L., Kleidman, R., et al.: Global evaluation of the Collection 5
777 MODIS darktarget aerosol products over land, *Atmospheric Chemistry and*
778 *Physics*, 10, 10399-10420, doi:10.5194/acp-10-10399-2010, 2010.

779 Levy, R., Remer, L., and Dubovik, O.: Global aerosol optical properties and
780 application to Moderate Resolution Imaging Spectroradiometer aerosol retrieval
781 over land, *Journal of Geophysical Research*, 112, 1-15, doi:
782 10.1029/2006JD007815, 2007.

783 Lim, Y.B., Tan, Y., Perri, M.J., Seitzinger, S.P., and Turpin, B.J.: Aqueous chemistry
784 and its role in secondary organic aerosol (SOA) formation, *Atmospheric*
785 *Chemistry and Physics*, 10, 10521-10539, doi: 10.5194/acp-10-10521-2010, 2010.

786 Liu, Y., Huang, J., Shi, G., Takamura, T., Khatri, P., Bi, J., Shi, J., Wang, T. Wang, X.,
787 and Zhang B.: Aerosol optical properties and radiative effect determined from
788 sky-radiometer over Loess Plateau of Northwest China, *Atmospheric Chemistry*
789 *and Physics*, 11, 11455–11463, doi: 10.5194/acp-11-11455-2011, 2011.

790 Liu, S., Hu, M., Slanina, S., He, L.Y., Niu, Y.W., Bruegemann, E., Gnauk, T. and
791 Herrmann, H.: Size distribution and source analysis of ionic compositions of
792 aerosols in polluted periods at Xinken in Pearl River Delta (PRD) of China,

793 Atmospheric Environment, 42, 6284-6295, doi: [http://dx.doi.org/10.1016/j.](http://dx.doi.org/10.1016/j.atmosenv.2007.12.035)
794 [atmosenv.2007.12.035](http://dx.doi.org/10.1016/j.atmosenv.2007.12.035), 2008.

795 Lu, Q., Zheng, J.Y., Ye, S.Q., Shen, X.L., Yuan, Z.B. and Yin, S.S.: Emission trends
796 and source characteristics of SO₂, NO_x, PM₁₀ and VOCs in the Pearl River Delta
797 region from 2000 to 2009, Atmospheric Environment, 46, 11-20, doi:
798 <http://dx.doi.org/10.1016/j.atmosenv.2012.10.062>, 2013.

799 Meng, Z., and Seinfeld, J.H.: On the source of the submicrometer droplet mode of
800 urban and regional aerosols, Aerosol Science and Technology, 20, 253- 265, doi:
801 [10.1080 /02786829408959681](http://dx.doi.org/10.1080/02786829408959681), 1994.

802 Myhre, G., et al.: Radiative forcing of the direct aerosol effect from AeroCom Phase
803 II simulations, Atmospheric Chemistry and Physics, 13, 1853-1877,
804 doi:[10.5194/acp-13-1853-2013](https://doi.org/10.5194/acp-13-1853-2013), 2013.

805 Morisette, J.T., Giglio, L., Csiszar, I. and Justice, C.O.: Validation of the MODIS
806 active fire product over Southern Africa with ASTER data, International Journal
807 of Remote Sensing, 26, 4239-4264, doi: [10.1080/01431160500113526](https://doi.org/10.1080/01431160500113526), 2005a.

808 Morisette, J.T., Giglio, L., Csiszar, I., Setzer, A., Schroeder, W., Morton, D. and
809 Justice, C.O.: Validation of MODIS active fire detection products derived from
810 two algorithms, Earth Interaction, 9, 1-23, doi: <http://dx.doi.org/10.1175/EI141.1>,
811 2005b.

812 Petrenko, M., Kahn, R., Chin, M., Soja, A., Kucsera, T., and Harshvardhan,: The use
813 of satellite-measured aerosol optical depth to constrain biomass burning emissions
814 source strength in the global model GOCART, Journal of Geophysical Research,

815 117, D18212, doi: 10.1029/2012JD017870, 2012.

816 Pierson, W.R., and Brachaczek, W.W.: Coarse and fine particle atmospheric nitrate
817 and HNO₃(g) in Claremont, California, during the 1985 nitrogen species methods
818 comparison study, *Atmospheric Environment*, 22, 1665–1668, doi:10.1016/
819 0004-6981(88)90394-0, 1998.

820 Pillai, P.S., and Moorthy, K.K.: Aerosol mass-size distributions at a tropical suburban
821 environment: response to mesoscale and synoptic processes, *Atmospheric
822 Environment*, 35, 4099- 4112, doi:10.1016/S1352-2310(01)00211-4, 2001.

823 Pio, C., Legrand, M., Oliveira, T., Afonso, J., Santos, C., Caseiro, A., Fialho, P.,
824 Barata, F., Puxbaum, H., Sanchez-Ochoa, A., Kasper-Giebl, A., Gelencsér, A.,
825 Preunkert, S., and Schock, M.: Climatology of aerosol composition (organic
826 versus inorganic) at nonurban sites on a west–east transect across Europe, *Journal
827 of Geophysical Research-Atmospheres*, 112, D23S02, 10.1029/2006JD008038,
828 2007.

829 Ramanathan, V., and Garnichael, G.: Global and regional climate changes due to
830 black carbon, *Nature Geoscience*, 1, 221-227, doi:10.1038/ngeo156, 2008.

831 Remer, L.A., Mattoo, S., Levy, R.C., Munchak, L.A.: MODIS 3km aerosol product:
832 algorithm and global perspective, *Atmospheric Measurement Techniques*, 6,
833 1829–1844, doi:10.5194/amt-6-1829-2013, 2013.

834 Remer, L., Kaufman, Y., Tanre, D., Mattoo, S., Chu, D.A., Martins, J.V., Li, R.R.,
835 Ichoku, C., Levy, R.C., Kleidman, R.G., Eck, T.F, Vermote, E. and Holben, B.N.:
836 The MODIS Aerosol Algorithms, Products, and Validation, *Jouranal of*

837 [Atmospheric Science, 62, 947-973, doi: 10.1175/JAS3385.1, 2005.](#)

838 Rosenfeld, D., Sherwood, S., Wood, R., and Donner, L.: Climate effects of aerosol-
839 cloud interactions, *Science*, 343, 379-380, doi: 10.1126/science.1247490, 2014.

840 Schuster, G.L., Dubovik, O., and Holben, B.N.: Angstrom exponent and bimodal
841 aerosol size distributions, *Journal of Geophysical Research*, 111, D07207, doi: 10.
842 1029 /2005JD006328, 2006.

843 Seinfeld, J., and Pandis, S.: *Atmospheric Chemistry and Physics: From Air Pollution*
844 *to Climate Change*, John Wiley & Sons, New York, 2006.

845 Situ, S.P, Guenther, A., Wang, X.M., Jiang, X.X., Turnipseed, A., Wu, Z.Y., Bai, J.H.,
846 and Wang, X.X.: Impacts of seasonal and regional variability in biogenic VOC
847 emissions on surface ozone in the Pearl River delta region, China, *Atmospheric*
848 *Chemistry and Physics*, 13, 11803- 11817, doi:10.5194/acp-13-11803-2013, 2013.

849 [Stelson, A.W. and Seinfeld, J.H.: Relative humidity and temperature dependence of](#)
850 [the ammonium nitrate dissociation constant, *Atmospheric Environment*, 16, 983-](#)
851 [992, doi:10.1016/0004-6981\(82\)90184-6, 1982.](#)

852 Stohl, A., Hittenberer, M., and Wotawa, G.: Validation of the Lagrangian particle
853 dispersion model Flexpart against large-scale tracer experiment data, *Atmospheric*
854 *Environment*, 32, 4245-4264, doi:10.1016/S1352-2310(98)00184-8, 1998.

855 Tao, J., Ho, K.F., Chen, L.G., Zhu, L.H., Han, J.L., and Xu, Z.C.: Effect of chemical
856 composition of PM_{2.5} on visibility in Guangzhou, China, 2007 Spring, *Particology*,
857 7, 68-75, doi: 10.1016/j.partic.2008.11.002, 2009.

858 Tsigaridis, K., et al.: The AeroCom evaluation and intercomparison of organic aerosol

859 in global models, *Atmospheric Chemistry and Physics*, 14, 10845-10895,
860 doi:10.5194/acp-14-10845-2014, 2014.

861 Volkamer, R., Ziemann, P.J., and Molina, M.J.: Secondary Organic Aerosol Formation
862 from Acetylene (C₂H₂): seedeffect on SOA yields due to organic photochemistry
863 in the aerosol aqueous phase, *Atmospheric Chemistry and Physics*, 9, 1907-1928,
864 doi: 10.5194/acp-9-1907-2009, 2009.

865 Wang, X.F., Wang, W.X., Yang, L.X., Gao, X.M., Nie, W., Yu, Y.C., Xu, P.J., Zhou, Y.,
866 and Wang, Z.: The secondary formation of inorganic aerosols in the droplet mode
867 through heterogeneous aqueous reactions under haze conditions, *Atmospheric*
868 *Environment*, 63, 68-76, doi: 10.1016/j.atmosenv.2012.09.029, 2012.

869 Wang, Z., et al.: Source and variation of carbonaceous aerosols at Mount Tai, North
870 China: results from a semi-continuous instrument, *Atmospheric Environment*, 45,
871 1655-1667, doi: 10.1016/j.atmosenv.2011.01.006, 2011.

872 Wang, Y., Zhuang, G.S., Tang, A.H., Yuan, H., Sun, Y.L., Chen, S. and Zheng, A.H.:
873 The ion chemistry and the source of PM_{2.5} aerosol in Beijing, *Atmospheric*
874 *Enviornment*, 39, 3771-3784, doi:10.1016/j.atmosenv.2005.03.013, 2005.

875 Yang, X. and Wenig, M.: Study of columnar aerosol size distribution in Hong Kong,
876 *Atmospheric Chemistry and Physics*, 9, 6175-6189, doi:10.5194/acp-9-6175-2009,
877 2009.

878 Yao, X.H., Ling, T.Y., Fang, M. and Chan, C.K.: Comparison of thermodynamic
879 predictions for in situ pH in PM_{2.5}, *Atmospheric Environment*, 40, 2835-2844,
880 doi:10.1016/j.atmosenv.2006.01.006, 2006.

881 Yao, X.H., Lau, A.P.S., Fang, M., Chan, C.K., and Hu, M.: Size distributions and
882 formation of ionic species in atmospheric particulate pollutants in Beijing, China:
883 2—dicarboxylic acids, *Atmospheric Environment*, 37, 3001-3007, doi:10.1016/
884 S1352-2310(03)00256-5, 2003a.

885 Yao, X.H., Fang, M. and Chan, C.K. The size dependence of chloride depletion in fine
886 and coarse sea-salt particles, *Atmospheric Environment*, 37, 742-751,
887 doi:10.1016/S1352-2310(02)00955-X, 2003b.

888 Yu, C., Chen, L.F., Li, S.S., Tao, J.H. and Su, L.: Estimating Biomass Burned Areas
889 from Multispectral Dataset Detected by Multiple-Satellite, *Spectroscopy and*
890 *Spectral Analysis*, 35, 739-745, doi:10.3964/j.issn.1000-0593(2015)03-0739 -07,
891 2015.

892 Zhang, Z.S., Engling, G., Zhang, L.M., Kawamura, K., Yang, Y.H., Tao, J., Zhang,
893 R.J., Chan, C.Y. and Li, Y.D.: Significant influence of fungi on coarse
894 carbonaceous and potassium aerosols in a tropical rainforest, *Environmental*
895 *Research Letters*, 10, 034015, doi:10.1088/1748-9326/10/3/034015, 2015.

896 Zhang, Z.S., Engling, G., Chan, C.Y., Yang, Y.H., Lin, M., Shi, S., He, J., Li, Y.D.,
897 and Wang, X.M.: Determination of isoprene-derived secondary organic aerosol
898 tracers (2-methyltetrols) by HPAEC-PAD: Results from size-resolved aerosols in a
899 tropical rainforest, *Atmospheric Environment*, 70, 468- 476, doi:10.1016/
900 j.atmosenv. 2013.01.020, 2013a.

901 Zhang, Q., Tie, X.X., Lin, W.L., Cao, J.J., Quan, J.N., Ran, L., and Xu, W.Y.:
902 Variability of SO₂ in an intensive fog in North China Plain: Evidence of high

903 solubility SO₂, Particuology, 11, 41-47, doi:10.1016/j.partic.2012.09.005, 2013b.

904 Zhao, Y.L., and Gao, Y.: Mass size distributions of water-soluble inorganic and
905 organic ions in size-segregated aerosols over metropolitan Newark in the US east
906 coast, Atmospheric Environment, 42, 4063-4078,
907 doi:10.1016/j.atmosenv.2008.01.032, 2008a.

908 Zhao, Y.L., and Gao, Y.: Acidic species and chloride depletion in coarse aerosol
909 particles in the US east coast, Science of The Total Environment, 407, 541- 547,
910 doi:10.1016/j.scitotenv.2008.09.002, 2008b.

911 Zheng, J.Y., He, M., Shen, X.L., Yin, S.S., and Yuan, Z.B.: High resolution of black
912 carbon and organic carbon emissions in the Pearl River Delta region, China,
913 Science of The Total Environment, 438, 189-200, doi: <http://dx.doi.org/10.1016/j.scitotenv.2012.08.068>, 2012.

914

915 Zheng, J.Y., Zhang, L.J., Che, W.W., Zheng, Z.Y. and Yin, S.S.: A highly resolved
916 temporal and spatial air pollutant emission inventory for the Pearl River Delta
917 region, China and its uncertainty assessment, Atmospheric Environment, 43,
918 5112- 5122, doi: <http://dx.doi.org/10.1016/j.atmosenv.2009.04.060>, 2009.

919 Zhou, S.Z., Davy, P.K., Wang, X.M., Cohen, J.B., Liang, J.Q., Huang, M.J., Fan, Q.,
920 Chen, W.H. Chang, M., Ancelet, T. and Trompeter, W.J.: High time-resolved
921 elemental components infine and coarse particles in the Pearl River Delta region
922 of Southern China: Dynamic variations and effects of meteorology, Science of the
923 Total Environment, doi: [10.1016/j.scitotenv.2016.05.194](https://doi.org/10.1016/j.scitotenv.2016.05.194), 2016 (in press).

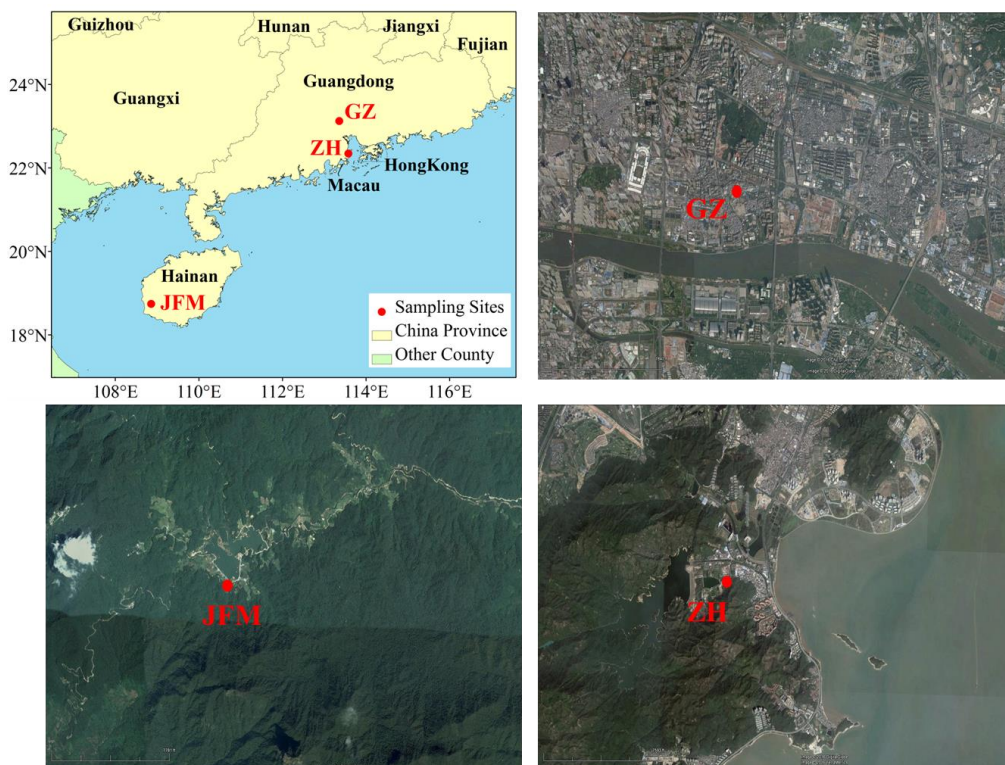
924 Zhou, Y., Xue, L.K., Wang, T., Gao, X.M., Wang, Z., Wang, X.F., Zhang, J.M., Zhang,

925 Q.Z., and Wang, W.X.: Characterization of aerosol acidity at a high mountain site
926 in central eastern China, *Atmospheric Environment*, 51, 11-20,
927 doi:10.1016/j.atmosenv.2012.01.061, 2012.

928 Zhuang, H., Chan, C.K., Fang, M., Wexler, A.S.: Size distributions of particulate
929 sulfate, nitrate and ammonium at a suburban site in Hong Kong, *Atmospheric*
930 *Environment*, 33, 843- 853, doi:10.1016/S1352-2310(98)00305-7, 1999.

931 **Figures**

932 **Figure 1.** Location of sampling sites in Southern China: GZ (Guangzhou), ZH
933 (Zhuhai), and JFM (Jianfeng Mountain) **and their surrounding environments**



934

935

936

937

938

939

940

941

942

943

944

945

946

947

948

949

950

951

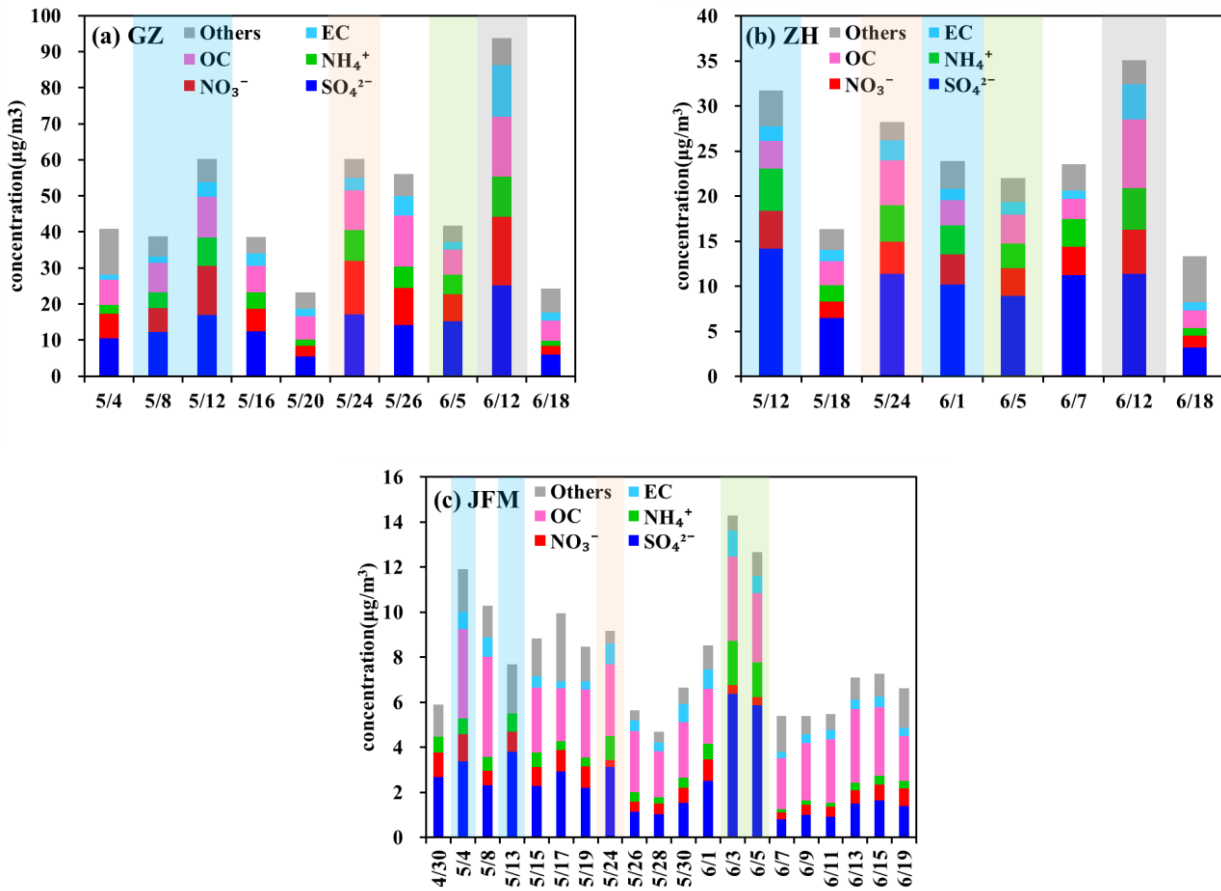
952

953

954

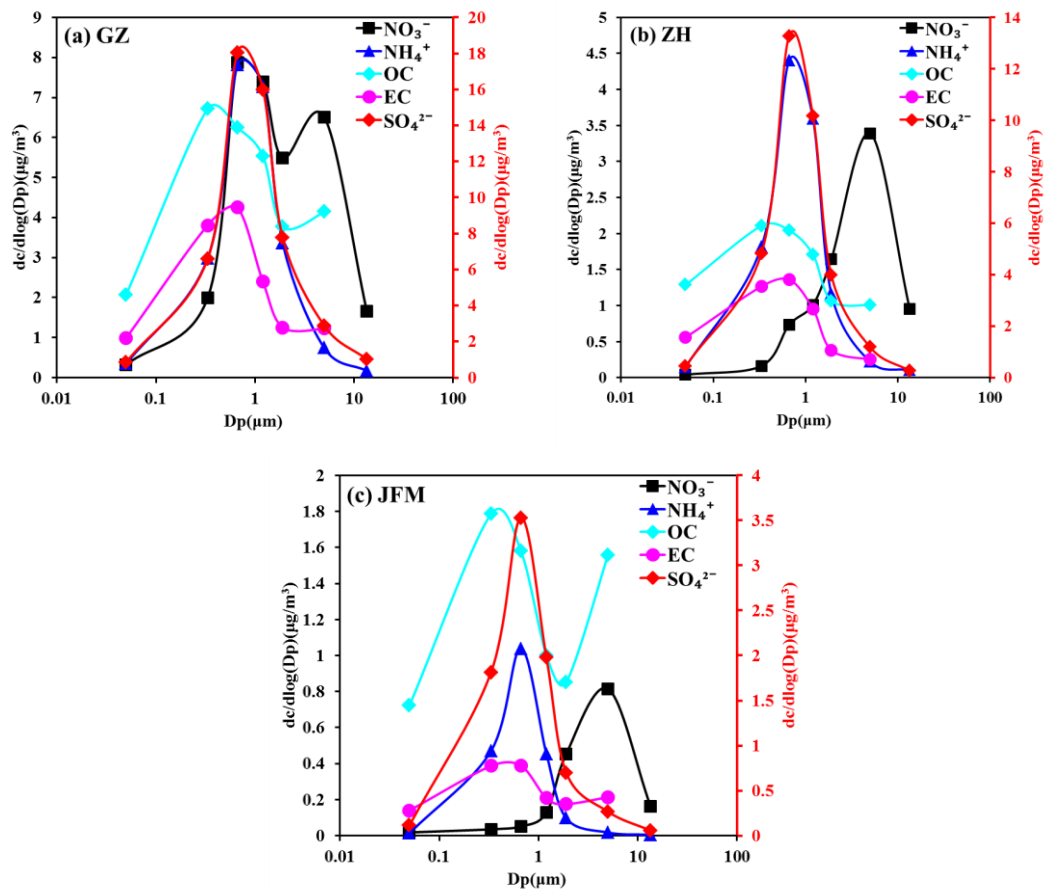
955

956 **Figure 2.** Time series of PM₁₈ chemical compositions at the three sites during the
 957 2010 wet season.



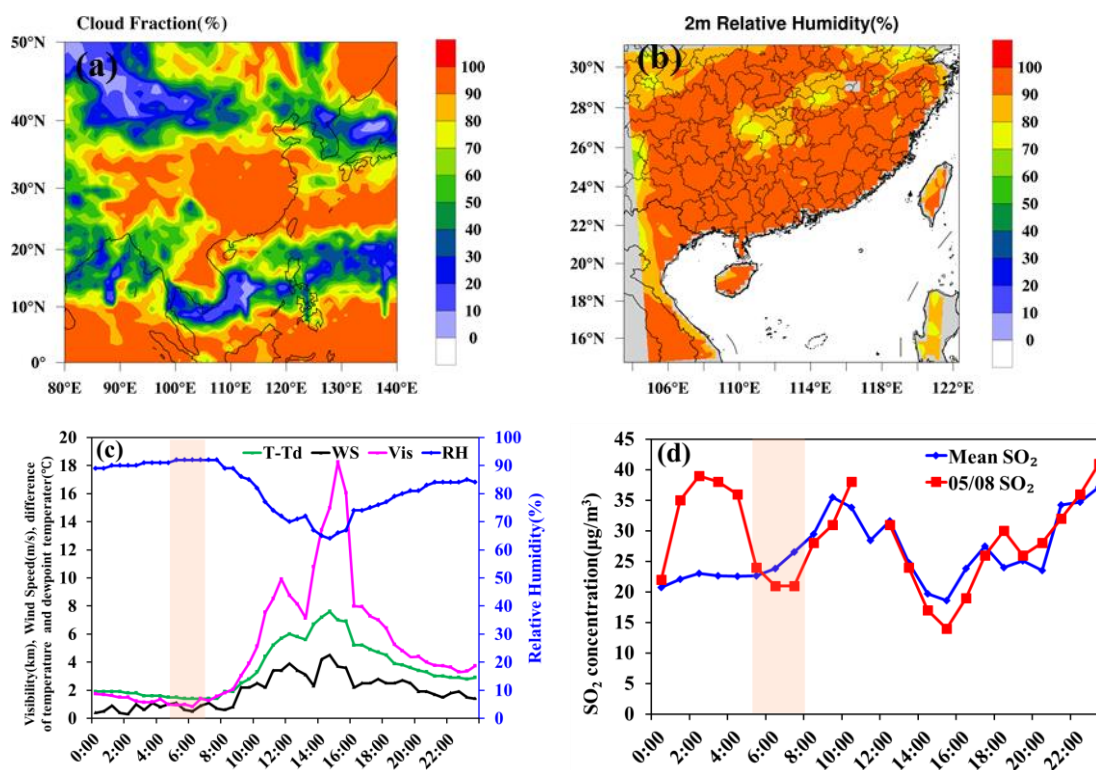
958
 959
 960
 961
 962
 963
 964
 965
 966
 967
 968
 969
 970
 971
 972
 973
 974
 975

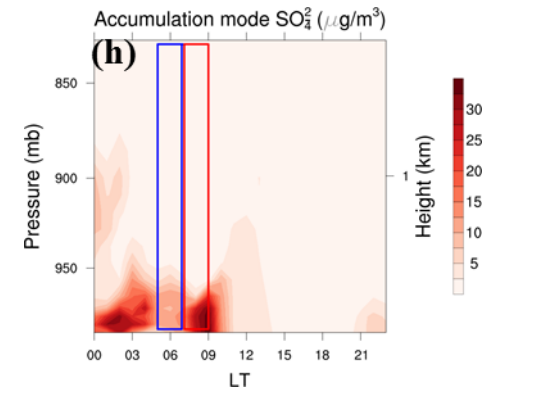
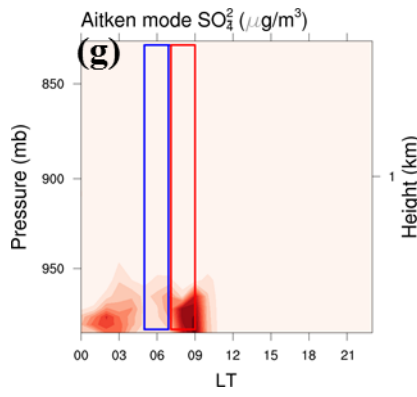
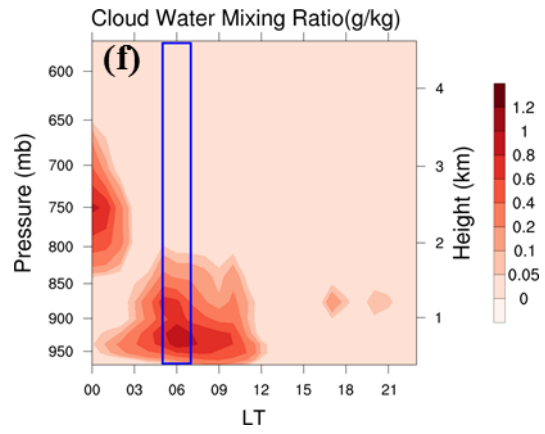
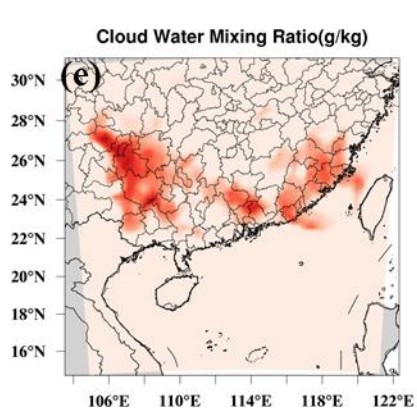
976 **Figure 3.** The mass size distribution of major compositions (SO_4^{2-} , NO_3^- , NH_4^+ , OC
 977 and EC) at the three sites during study period (SO_4^{2-} is plotted against the right
 978 Y-Axes)



979

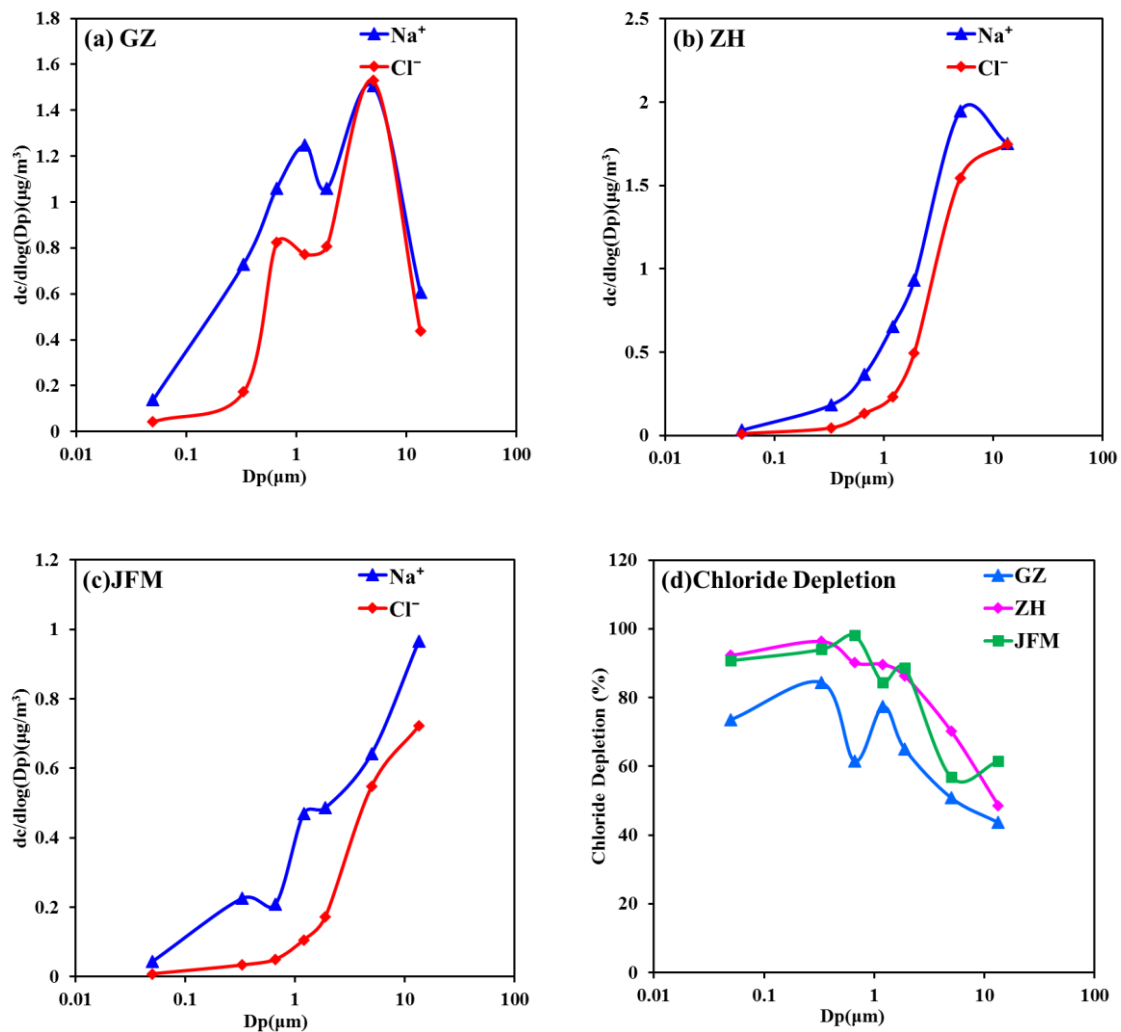
980 **Figure 4.** Case study on 8th May. in GZ ((a)The cloud fraction over Southern China;
 981 (b)Distribution of simulated average 2 m relative humidity at 05:00-07:00 LT; (c) The
 982 time series of observational visibility, wind speed, relative humidity and the
 983 depression of dew point (time resolution was 30mins); (d) The time series of
 984 monitored mean SO₂ during 2009-2010 and SO₂ on 8th May ;(e) Distribution of
 985 simulated average cloud; (f) The time-height distribution of simulated cloud water
 986 mixing ratio on 8th May; (g-h) The time-height of simulated Aitken and accumulation
 987 mode SO₄²⁻)





988

989 **Figure 5.** The mass size distribution of (a-c) Na^+ and Cl^- and (d) percentage of
 990 chloride depletion at the three sites



991

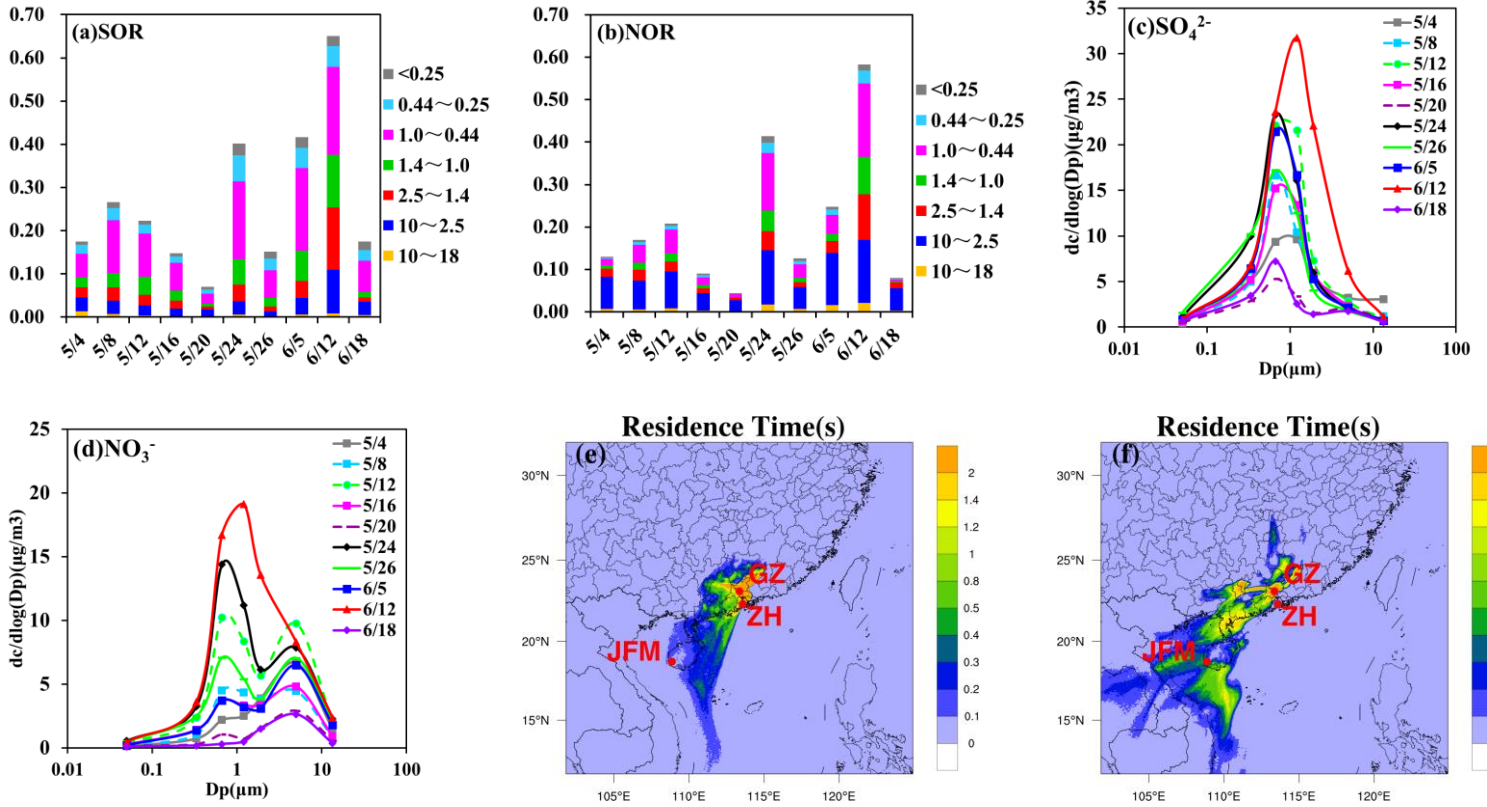
992

993

994 **Figure 6.** Case study on 12th Jun. in GZ ((a-b) The time series of SOR and NOR; (c-d)

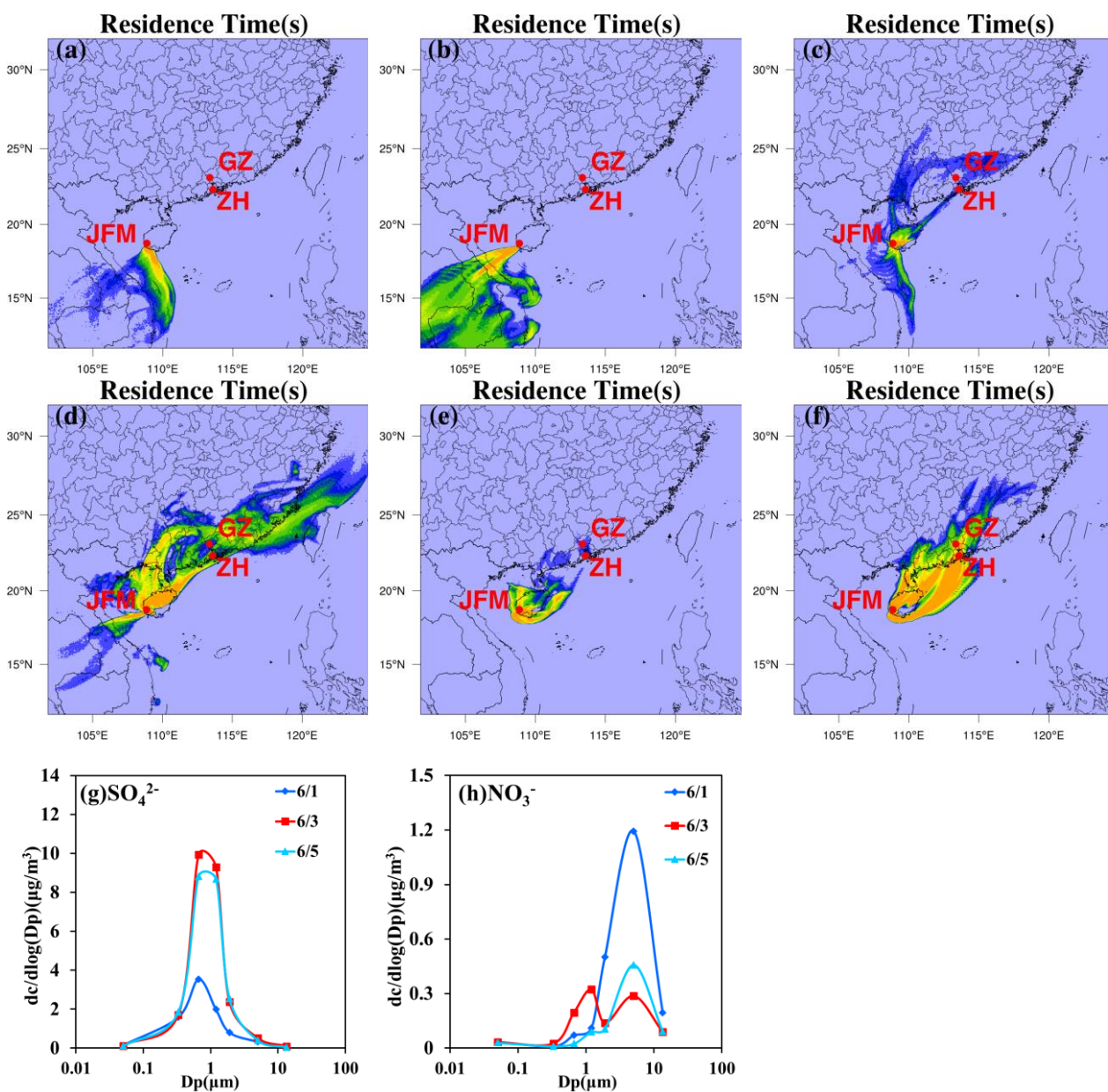
995 The mass size distribution of SO₄²⁻ and NO₃⁻; (e-f) FLEXPART-WRF total column

996 residence times over the last 72h arriving in GZ on 12th Jun. at 100m and 1000m



997

998 **Figure 7.** Case study on 1st, 3rd and 5th Jun. in JFM ((a-b) FLEXPART-WRF total
 999 column residence times on over the last 72h arriving in JFM on 1st Jun. at 100m and
 1000 1000m; (c-d) and (e-f) same at (a-b) but on 3rd and 5thJun. respectively; (g-h) The
 1001 mass size distribution of SO₄²⁻ and NO₃⁻)

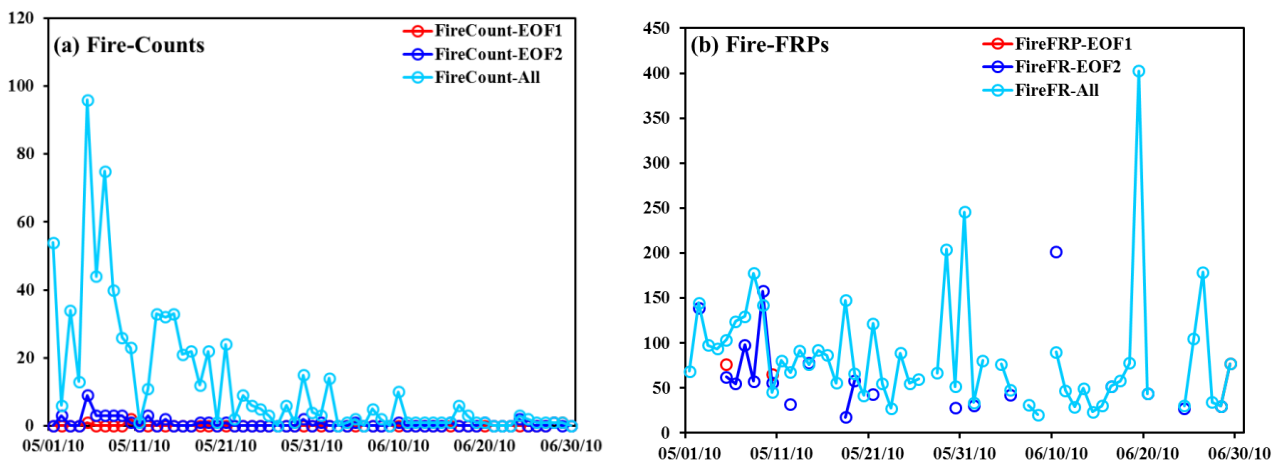


1002

1003

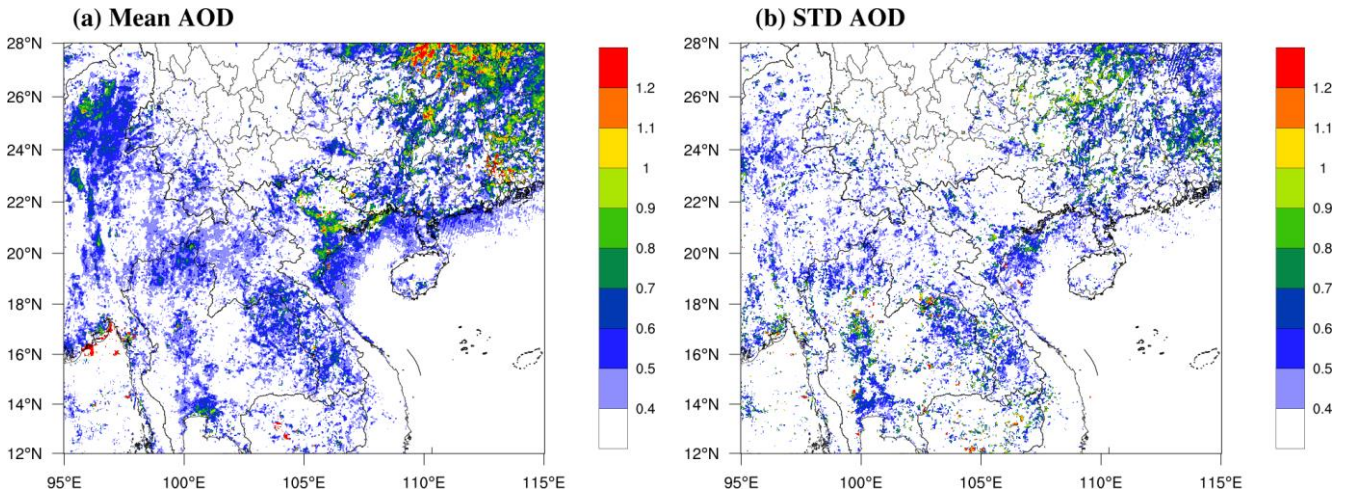
1004

1005 **Figure 8.** Spatially averaged/aggregated statistics of (a) MODIS Fire numbers (Count)
 1006 and (b) Fire Radiative Power (FRP) over Southeast Asia for May and June 2010. The
 1007 statistics represent the respective Count [total number of burning 1kmx1km pixels]
 1008 and average FRP [W/m^2 per 1kmx1km pixel] over the whole of Southeast Asia and
 1009 the specific regions where the AOD (as an indicator for smoke) has its highest levels
 1010 of variability: EOF1 and EOF2.



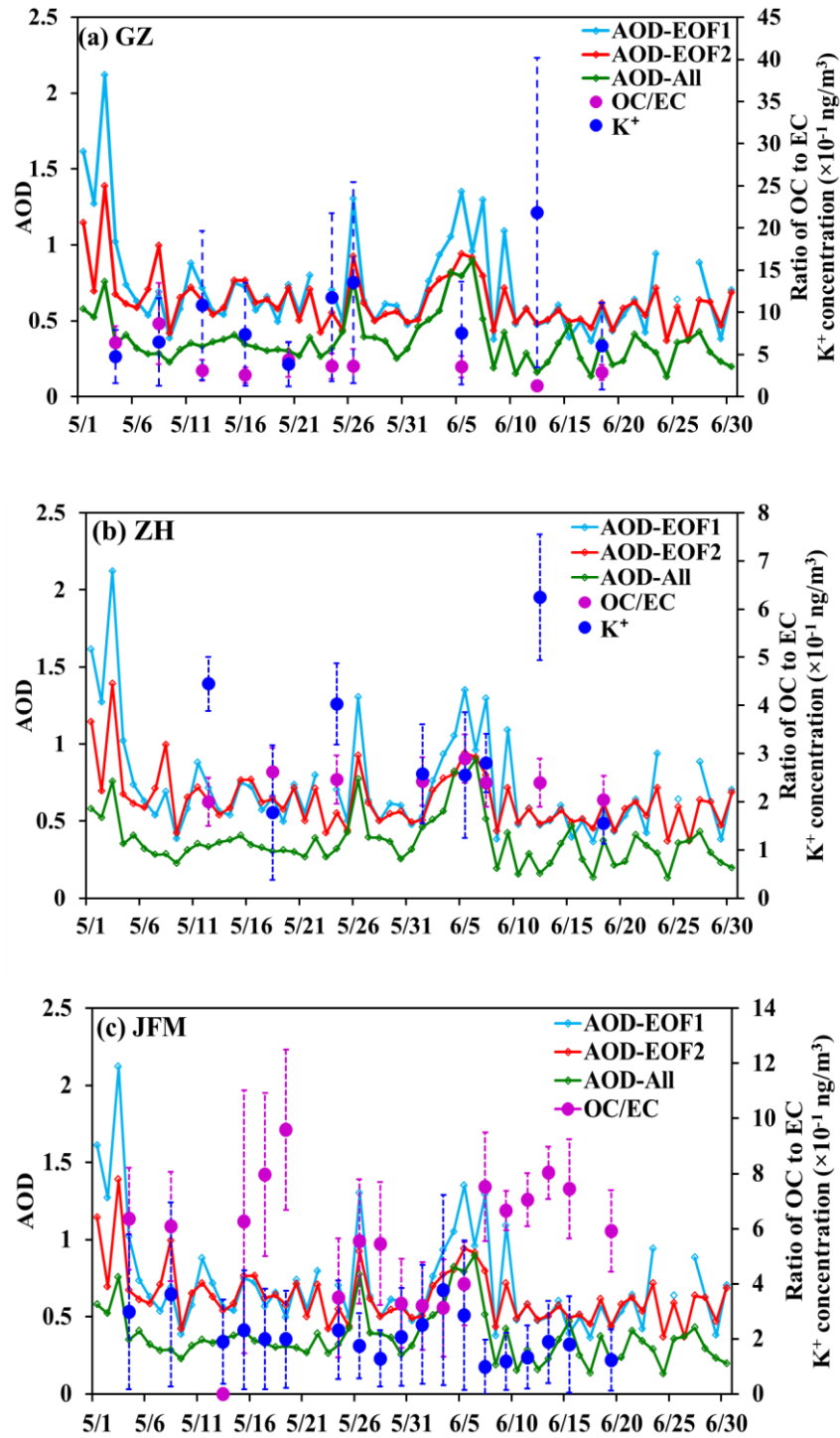
1011
 1012
 1013
 1014
 1015
 1016
 1017
 1018

1019 **Figure 9.** Average spatial distribution of the (a) mean and (b) standard deviation of
1020 daily MODIS AOD from May 1st through June 30th 2010



1021
1022
1023
1024
1025
1026
1027
1028
1029
1030
1031
1032
1033

1034 **Figure 10.** The time-varying statistics of the AOD averaged over the first two EOFs
 1035 of the AOD (reflecting the regions most impacted by AOD variance or smoke from
 1036 fires) and the average K^+ concentration and average ratio of OC/EC in the three sites.



1037

1038 **Tables**

1039 **Table 1.** Average concentration and standard deviation [$\mu\text{g m}^{-3}$] of chemical
 1040 components in the given size-resolved particles (and their percentage of PM_{10}) at the
 1041 three sites during the 2010 wet season.

Site	Size	Sum of measured species	SO_4^{2-}	NO_3^-	NH_4^+	OC	EC
GZ	$\text{PM}_{1.0}$	24.4 ± 10.9	8.0 ± 3.1 (60.2)	3.0 ± 2.4 (34.5)	3.4 ± 1.7 (64.2)	5.5 ± 2.0 (57.9)	2.9 ± 2.6 (72.5)
	$\text{PM}_{2.5}$	34.9 ± 17.3	11.7 ± 5.2 (88.0)	5.0 ± 4.0 (57.5)	4.9 ± 2.9 (92.5)	7.2 ± 2.7 (75.8)	3.4 ± 3.2 (85.0)
	PM_{10}	46.7 ± 20.6	13.3 ± 5.8	8.7 ± 5.2	5.3 ± 3.1	9.5 ± 3.7	4 ± 3.8
ZH	$\text{PM}_{1.0}$	12.9 ± 4.5	6.3 ± 2.1 (66.3)	$0.3 \pm 0.$ 3(10.3)	2.2 ± 0.8 (71.0)	2.4 ± 1.1 (66.7)	1.3 ± 0.8 (76.5)
	$\text{PM}_{2.5}$	18.1 ± 6.8	8.8 ± 3.2 (92.6)	0.9 ± 0.8 (31.0)	3.0 ± 1.2 (96.8)	3.0 ± 1.5 (83.3)	1.5 ± 0.9 (88.2)
	PM_{10}	23.7 ± 7.3	9.5 ± 3.4	2.9 ± 1.1	3.1 ± 1.3	3.6 ± 1.9	1.7 ± 1.0
JFM	$\text{PM}_{1.0}$	4.4 ± 1.6	1.8 ± 1.0 (75.0)	0.1 ± 0.1 (16.7)	0.5 ± 0.3 (83.3)	1.5 ± 0.7 (57.7)	0.3 ± 0.2 (60.0)
	$\text{PM}_{2.5}$	5.8 ± 2.3	2.2 ± 1.5 (91.7)	0.2 ± 0.1 (33.3)	0.6 ± 0.5 (99.0)	1.8 ± 0.8 (69.2)	0.4 ± 0.2 (80.0)
	PM_{10}	8.0 ± 2.6	2.4 ± 1.5	0.6 ± 0.3	0.6 ± 0.5	2.6 ± 1.1	0.5 ± 0.3

1042 **Table 2.** Statistical parameters of samples with air masses from ocean

Site	Date	Droplet	Percentage	T (°C)	RH (%)	P (hPa)	WS (m s ⁻¹)	Low
		mode sulfate (µg m ⁻³)	of sulfate in droplet mode (%)					Cloud cover (%)
GZ	2010/5/8	7.4	61	27.5	82.0	997.1	1.9	70
	2010/5/12	11.1	65	25.0	77.5	1002.9	1.5	60
ZH	2010/5/12	9.5	67	24.9	83.0	1006.1	3.4	70
	2010/6/1	6.8	67	24.8	80.0	1002.0	5.1	70
JFM	2010/5/4	2.2	64	22.0	83.0	916.9	1.0	70
	2010/5/13	2.5	67	23.7	75.8	918.3	1.8	70

1043